THE JOURNAL OF BIOLOGICAL CHEMISTRY VOL. 291, NO. 25, pp. 13335–13348, June 17, 2016


# Central Mechanisms Mediating Thrombospondin-4-induced Pain States*

Received for publication, February 23, 2016, and in revised form, April 15, 2016 Published, JBC Papers in Press, April 19, 2016, DOI 10.1074/jbc.M116.723478

**John Park[‡1,2], Yanhui Peter Yu[‡1], Chun-Yi Zhou[‡1], Kang-Wu Li[§], Dongqing Wang[¶], Eric Chang[§3], Doo-Sik Kim[§], Benjamin Vo[§], Xia Zhang[§], Nian Gong[§], Kelli Sharp[‖], Oswald Steward[‖], Iuliia Vitko[**], Edward Perez-Reyes[**], Cagla Eroglu[‡‡], Ben Barres[¶¶], Frank Zaucke[‖‖], Guoping Feng[¶], and Z. David Luo[‡§‖4]**

*From the [‡]Department of Pharmacology and [§]Department of Anesthesiology and Perioperative Care, University of California, Irvine, California 92697, [¶]Department of Brain and Cognitive Sciences, Massachusetts Institute of Technology, Cambridge, Massachusetts 02139, [‖]Reeve-Irvine Research Center, University of California, Irvine, School of Medicine, Irvine, California 92697, [**]Department of Pharmacology, University of Virginia School of Medicine, Charlottesville, Virginia 22908, [‡‡]Cell Biology, Duke University Medical Center, Durham, North Carolina 27710, [¶¶]Department of Neurobiology, Stanford University, Stanford, California 94305, and [‖‖]Center for Biochemistry and Cologne Center for Musculoskeletal Biomechanics, Medical Faculty, University of Cologne, D50931 Cologne, Germany*

**Peripheral nerve injury induces increased expression of thrombospondin-4 (TSP4) in spinal cord and dorsal root ganglia that contributes to neuropathic pain states through unknown mechanisms. Here, we test the hypothesis that TSP4 activates its receptor, the voltage-gated calcium channel $Ca_v\alpha_2\delta_1$ subunit ($Ca_v\alpha_2\delta_1$), on sensory afferent terminals in dorsal spinal cord to promote excitatory synaptogenesis and central sensitization that contribute to neuropathic pain states. We show that there is a direct molecular interaction between TSP4 and $Ca_v\alpha_2\delta_1$ in the spinal cord *in vivo* and that TSP4/$Ca_v\alpha_2\delta_1$-dependent processes lead to increased behavioral sensitivities to stimuli. In dorsal spinal cord, TSP4/$Ca_v\alpha_2\delta_1$-dependent processes lead to increased frequency of miniature and amplitude of evoked excitatory post-synaptic currents in second-order neurons as well as increased $VGlut_2$- and PSD95-positive puncta, indicative of increased excitatory synapses. Blockade of TSP4/$Ca_v\alpha_2\delta_1$-dependent processes with $Ca_v\alpha_2\delta_1$ ligand gabapentin or genetic $Ca_v\alpha_2\delta_1$ knockdown blocks TSP4 induced nociception and its pathological correlates. Conversely, TSP4 antibodies or genetic ablation blocks nociception and changes in synaptic transmission in mice overexpressing $Ca_v\alpha_2\delta_1$. Importantly, TSP4/$Ca_v\alpha_2\delta_1$-dependent processes also lead to similar behavioral and pathological changes in a neuropathic pain model of peripheral nerve injury. Thus, a TSP4/$Ca_v\alpha_2\delta_1$-dependent pathway activated by TSP4 or peripheral nerve injury promotes exaggerated presynaptic excitatory input and evoked sensory neuron hyperexcitability and excitatory synaptogenesis, which together lead to central sensitization and pain state development.**

Neuropathic pain due to peripheral nerve injury is associated with up-regulation of expression of thrombospondin-4 (TSP4)[5] in spinal cord and dorsal root ganglia (DRG) that induces increased frequency of miniature excitatory post-synaptic currents (mEPSC) in dorsal spinal cord and neuropathic pain states (1, 2). Details about the mechanisms remain to be defined however. TSP4 belongs to a five-member thrombospondin superfamily of oligomeric, extracellular matrix glycoproteins (TSP1–5) that can be subdivided into groups A (TSP1/2) and B (TSP3/4/5) based on structure and functional domain similarities (3). TSP proteins are important in mediating cell-to-cell and cell-to-matrix interactions (3, 4). TSP4 is expressed in multiple sites, and its functions are not well defined (5) although there is evidence that TSP4 promotes neurite outgrowth (6).

Recently, TSPs have been shown to regulate early excitatory synaptogenesis in the brain by interacting with its receptor, the voltage-gated calcium channel $\alpha_2\delta_1$ subunit ($Ca_v\alpha_2\delta_1$) proteins (7, 8). The $Ca_v\alpha_2\delta$ subunit family of the voltage-gated calcium channels includes four $Ca_v\alpha_2\delta$ subunits ($Ca_v\alpha_2\delta_{1-4}$) encoded by different genes (9–11). $Ca_v\alpha_2\delta$ functions include trafficking and stabilizing voltage-gated calcium channel to the plasma membrane and pre-synaptic terminals (12–14), fine-tuning channel functions, and gating properties (13, 15, 16).

Importantly, $Ca_v\alpha_2\delta_1$ and $Ca_v\alpha_2\delta_2$ subunits are binding sites of gabapentinoids (17, 18), which have anti-neuropathic pain efficacy in patients (19–22) and animal models (23–26). $Ca_v\alpha_2\delta_1$, but not $Ca_v\alpha_2\delta_2$, is up-regulated in sensory neurons after peripheral nerve injury (27, 28), leading to increased

* This work was supported, in part, through access to the confocal facility of the Optical Biology Shared Resource of the Cancer Center, Support Grant CA-62203, at the University of California Irvine and by National Institutes of Health Grants NS069524 (to E. P.-R.), NS40135, DE014545, and NS064341 (to Z. D. L.), and DE021847 (to O. S. and Z. D. L).The authors declare that they have no conflicts of interest with the contents of this article. The content is solely the responsibility of the authors and does not necessarily represent the official views of the National Institutes of Health.

[1] These authors contributed equally to the work.

[2] Recipient of a Pre-Doctoral Fellowship in Pharmacology/Toxicology from the Pharmaceutical Research and Manufacturers of America Foundation (PRMAF-52427).

[3] Recipient of National Institutes of Health Rehabilitation Medicine Scientist Training Program fellowship (K-12) and faculty career development (KL-2) fellowship from the Institute for Clinical and Translational Science.

[4] To whom correspondence should be addressed: Dept. of Anesthesiology and Perioperative Care, University of California Irvine, Gillespie Bldg., Rm. 3113, 837 Health Sci. Rd., Irvine, CA 92697. Tel.: 949-824-7469; Fax: 949-824-7447; E-mail: zluo@uci.edu.

[5] The abbreviations used are: TSP4, thrombospondin-4; DRG, dorsal root ganglia; mEPSC, miniature excitatory post-synaptic current(s); eEPSC, evoked excitatory post-synaptic current(s); TG, transgenic; CKO, conditional knock-out; SNL, spinal nerve ligation; AAV, adeno-associated virus; scAAV, self-complementary recombinant AAV; PWT, paw withdrawal thresholds; ANOVA, analysis of variance; IP, immunoprecipitation; i.t., intrathecal.

$Ca_v\alpha_2\delta_1$ axonal transport to the central presynaptic terminals of sensory neurons in dorsal spinal cord (27, 29). Similar to injury-induced TSP4, injury-induced $Ca_v\alpha_2\delta_1$ also has been shown to increase mEPSC frequency in neurons of dorsal spinal cord, which may contribute to central sensitization and neuropathic pain states (24, 25, 27, 29–31, 33).

Collectively, these observations suggest the following intriguing hypothetical mechanistic model: 1) peripheral nerve injury up-regulates $Ca_v\alpha_2\delta_1$ in peripheral sensory neurons and its central terminals; 2) peripheral nerve injury also triggers increased synthesis and release of TSP4 in spinal cord and DRG; 3) increased TSP4 interacts directly with its receptor $Ca_v\alpha_2\delta_1$ on the central terminals of sensory neurons to increase excitatory synaptogenesis and synaptic neurotransmission; 4) increased excitatory transmission in dorsal spinal cord contributes to central sensitization and neuropathic pain development. This model leads to several predictions. First, there should be direct molecular interactions between TSP4 and $Ca_v\alpha_2\delta_1$ in the adult spinal cord *in vivo*. Second, if TSP4 and $Ca_v\alpha_2\delta_1$ are mechanistically linked, then manipulations of one protein should alter the development of pain states induced by manipulations of the other protein. Here, we tested critical aspects of this model and the underlying mechanisms.

## Materials and Methods

### *Mouse Genetics*

The $Ca_v\alpha_2\delta_1$ overexpressing transgenic (TG) mice were generated as described previously (34). TSP4 knock-out (KO) mice were from The Jackson Laboratory (Bar Harbor, ME). The $Ca_v\alpha_2\delta_1$ TG/TSP4 KO double mutant mice and their control littermates were bred internally. The $Ca_v\alpha_2\delta_1$ conditional knock-out (CKO) mice were generated by floxing exon 6 of the $Ca_v\alpha_2\delta_1$ gene (MGI (Mouse Genomics Informatics) ID 88295) with loxP sites. Homozygous $Ca_v\alpha_2\delta_1$ CKO mice were crossed with the Advillin-Cre mice with Cre recombinase expression only in Advillin-positive sensory neurons (35) to generate heterozygous $CKO^{Adv\text{-}Cre+/-}$ mice, which were used to generate homozygous $CKO^{Adv\text{-}Cre+/-}$ mice for experiments. Mouse genotyping was performed by TransnetYX, Inc. (Cordova, TN). All the mice appeared normal with respect to grooming, social interactions, and feeding and showed no signs of abnormality or any obvious motor defects, tremor, seizure, or ataxia. Only adult male mice were used for the experiments. All animal care and experiments were performed according to protocols approved by the Institutional Animal Care Committee of the University of California, Irvine.

### *Expression and Purification of Recombinant TSP4*

Human embryonic kidney cell line 293-EBNA (Invitrogen) in DMEM/F-12 medium (Mediatech, Manassas, VA) was transfected with recombinant rat TSP4 with N-terminal His tag using the calcium phosphate transfection method, then transfected cells were selected with 0.5 $\mu$g/ml puromycin. Secreted TSP4 was confirmed by Western blots using anti-Tetra-His monoclonal antibodies (catalog #34670, negligible cross-reactivity with mammalian and other species cell lysates validated by Qiagen, Valencia, CA). The His-tagged proteins were purified using a nickel-nitrilotriacetic acid column based on the manufacturer's instructions (Invitrogen), concentrated and buffer-exchanged to PBS with Amicon Ultra-4 Centrifugal Filter Unit (50K molecular weight cutoff; Millipore, Billerica, MA), aliquoted, and stored at −80 °C until use.

### *Immunoprecipitation*

The spinal cord tissues from adult male mice and adult male Harlan Sprague-Dawley rats were collected by hydraulic extrusion from animals deeply anesthetized with isoflurane and lysed in protein extraction buffer (50 mM Tris buffer, pH 8.0, 0.1% Triton X-100, 150 mM NaCl, 1 mM EDTA, and protease inhibitors). The cell lysate was then incubated on ice for 15 min, centrifuged $\times$20,000 $\times$ *g* for 20 min at 4 °C. The supernatant was incubated with anti-TSP4 polyclonal antibody (guinea pig, 1:750, validated previously; Ref. 36) overnight at 4 °C. Protein A/G-agarose beads (Thermo, Waltham, MA) were then added, incubated for 2 h at 4°C, and washed with protein extraction buffer. The antibody-captured proteins were eluted in non-reducing condition with low pH elution buffer (Thermo, Waltham, MA) at room temperature, and the same volume of control supernatant or immunocomplex samples was analyzed by Western blots under non-reducing conditions.

### *Solid-phase Binding*

Briefly, FLAG-$Ca_v\alpha_2\delta_1$cDNA was transiently transfected into the tsA-201 cell line stably expressing Cav2.2 and Cav$\beta$3 (a gift from Dr. D. Lipscombe from Brown University (37) by Lipofectamine 2000 (Invitrogen). The transfected cells were washed and extracted in protein extraction buffer (50 mM Tris, 150 mM NaCl, 1 mM EDTA, 0.1% Triton-X, pH 7.4) in 2–3 days. The cell lysate was incubated on ice for 15 min, then centrifuged $\times$13,000 $\times$ *g* at 4 °C for 20 min. The supernatant was rotating-incubated with anti-FLAG M2 agarose affinity resin (Sigma) for 2 h at 4 °C and washed with protein extraction buffer. FLAG-$Ca_v\alpha_2\delta_1$ was eluted in elution buffer (0.1 M glycine, pH 3.5) and stored at −20 °C until use.

The reagents for solid-phase binding were from Invitrogen. Recombinant TSP4 proteins (80 $\mu$g/ml) were immobilized onto a 96-well polystyrene plates (Thermo, Waltham, MA) overnight at 4 °C in coating buffer A. All further incubations were carried out at room temperature for 1 h, and proteins or antibodies were diluted in assay buffer containing bovine serum albumin (BSA). After washing and blocking, the plates were incubated with FLAG-$Ca_v\alpha_2\delta_1$, washed, then incubated with mouse monoclonal anti-FLAG antibodies (1:1000; catalog #F1804, validated against FLAG fusion proteins by Sigma) followed by horseradish peroxidase (HRP)-conjugated secondary antibodies. The bound FLAG-$Ca_v\alpha_2\delta_1$ complexes were detected by measuring a color reaction at 450 nm after adding tetramethylbenzidine for 15 min followed by adding sulfuric acid to stop the reaction.

### *Surface Plasmon Resonance Binding (38)*

All experiments were carried out using BIAcore 3000 and CM5 Sensor Chip (GE Healthcare) at 25 °C. $Ca_v\alpha_2\delta_1$antibody (mouse, catalog #D219, Sigma) was coupled to the dextran matrix of a CM5 sensor chip using Amine Coupling kit as described (39). The antibody specificity for $Ca_v\alpha_2\delta_1$ was con-

firmed with tissue samples from $Ca_v\alpha_2\delta_1$knock-out mice (Fig. 4*C*). Excess reactive esters were quenched by injection of 1.0 M ethanolamine-hydrochloride, pH 8.5. The binding assays were performed using HBS-P buffer (0.01 M HEPES, pH 7.4, 0.15 M NaCl, 0.005%, and surfactant P20) as running buffer. Purified TSP4 proteins and $Ca_v\alpha_2\delta_1$ protein extracts from tsA-201 cells stably expressing $Ca_V2.2e$ (Δ24a, 31a), $Ca_V\beta_3$, and $Ca_v\alpha_2\delta_1$ as described (40) were diluted in HBS-P buffer (GE Healthcare). $Ca_v\alpha_2\delta_1$ protein extracts were injected at a flow rate of 10 μl/min over the immobilized $Ca_v\alpha_2\delta_1$ antibody flow cells followed by injection of purified TSP4 proteins at a flow rate of 20 μl/min. Nonspecific binding of TSP4 to the flow cell without immobilized $Ca_v\alpha_2\delta_1$ antibody was subtracted from all binding curves using BIAevaluation software (version 3.0, GE Healthcare) and plotted using Graphpad Prism (Graphpad Software, San Diego, CA).

### *Spinal Nerve Ligation (SNL) (41)*

Briefly, the left L4 spinal nerve of mice, which is equivalent to L5 spinal nerve in rats (42), was exposed in isoflurane-anesthetized animals and tightly ligated between the DRG and their conjunction to form the sciatic nerve with a silk suture. Sham procedures were done in the same way without spinal nerve ligation. Behavioral tests were performed at designated times before collection of tissue samples, which were either processed immediately for biochemical studies or kept at −80 °C until use.

$Ca_v\alpha_2\delta_1$ shRNA design and delivery via an adeno-associated viral vector (scAAV). A cDNA encoding the complete coding sequence of the mouse $Ca_v\alpha_2\delta_1$ subunit was obtained from Open Biosystems (IMAGE: 40061614), then cloned into a mammalian expression vector (pYFP-C1, Clontech). Candidate shRNAs were designed using publicly available web tools (Invitrogen Block-it and Genscript). These shRNAs were imbedded in a mir30 backbone using opposing BsmBI sites to insert complementary oligonucleotides encoding the shRNAs without altering the miR sequence (43, 44). The shRNAs were cloned into a human H1 promoter amplified from pLVUTH (Addgene clone 11650). We engineered a novel scAAV using the pLVUTH backbone and the δ-ITR sequences described by McCarty *et al.* (45). This vector uses a CMV enhanced human synapsin-1 promoter (46) to drive the expression of mCherry (provided by Dr. Roger Y. Tsien, UCSD) that was modified by adding the C-terminal ER export signal (FCYENE) from Kir2.1 (47). Four shRNAs were screened for target knockdown after expression in HEK-293 cells. Knockdown efficiency was measured using quantitative PCR with primers that encompassed the shRNA binding site (48). The shRNA with the highest knockdown efficacy (80%) relative to a scrambled control was AD1: AACTGGACAAGTGCCTTAGAT. CSRH1AD1 scAAV particles pseudotyped with serotype 8 were purified by the University of North Carolina Vector Core (titer $2 \times 10^{12}$ virus molecules/ml).

### *Intrathecal Injection*

Intrathecal injections between lumbar L5/6 regions for rats or L4/5 regions for mice were performed under light isoflurane anesthesia through a 30-gauge needle connected to a microinjector (Tritech Research, Inc., Los Angeles, CA). A total volume of 10 μl per rat or 5 μl per mouse was injected.

### *Behavioral Test*

Testing was performed in a blinded fashion. Behavioral test values between left and right hind paws from the SNL groups were recorded separately and used for statistical analysis, and that from non-SNL groups were averaged and used for statistical analysis.

*Tactile Allodynia*—Hind paw sensitivities to von Frey filament stimulation were tested for tactile allodynia as described previously (2, 49, 50). After acclimatization in wire mesh-floored transparent enclosures, the animals were accessed for the 50% paw withdrawal thresholds (PWT) to von Frey filament (Stoelting Wood Dale) stimulation using the up-down method (51). Briefly, the plantar surface of the hind paw was contacted perpendicularly with the first filament (2.0 g for rats or 0.41 g for mice) until it was slightly bent. A positive response of paw lifting within 5 s led to the use of the next lighter filament, and a negative response led to the use of the next heavier filament until a total of six measurements had been made, starting from the one before any change in the behavioral response. A score of 15 g for rats or 3 g for mice was assigned if five consecutive negative responses had occurred or a score of 0.25 g for rats or 0.01 g for mice was assigned if four consecutive positive responses had occurred. The data were then used to determine the 50% response threshold described previously (25).

*Thermal Hyperalgesia*—Reduced hind paw withdrawal latency to thermal stimuli was measured using a Hargreaves (hot box) apparatus (University of California San Diego, CA) (52) as the indication of thermal hyperalgesia. After acclimatization for at least 30 min on a glass floor maintained at 30 ± 0.1 °C in transparent enclosures, the hind paw plantar surface of a free-moving animal was stimulated by radiant heat projecting from a high intensity light bulb through a small aperture below the glass surface. When the animal moved the paw away from the thermal stimulus, motion detectors on the apparatus turned off the heating light automatically. The paw withdrawal latency was recorded as the time between thermal stimulus application and hind paw withdrawal. 20 s were set as the cutoff time to prevent thermal injury or skin sensitization. Two readings per paw were averaged for statistical analysis.

*Mechanical Hyperalgesia*—After acclimatization for 1 week to human holding and touch, rats were tested for mechanical hyperalgesia (Randall-Selitto Test (53) using a Paw Pressure Analgesymeter (Ugo Basil North America)). Briefly, a rat hind paw was placed between a blunt pointer and a flat surface and subjected to an escalating force (16 g/s) until paw withdrawal by the animal. The recorded hind paw withdrawal inducing force was used as the paw pressure withdrawal thresholds.

*Locomotor Function Tests*—After acclimatization daily for 1 week to human handling and the open field test apparatus, mice were tested for locomotor function by a blinded observer using scores of 0–9 arranging from no ankle movement (0) to frequent or consistent coordinated plantar stepping, normal trunk stability, and tail up position (9) as described by Basso *et al.* (54).

### *Western Blots*

Briefly, equal amounts of proteins were separated in 3–8% NuPAGE Tris acetate gels (Invitrogen) by electrophoresis, then transferred to polyvinylidene difluoride membranes electrophoretically. After blocking nonspecific binding sites with 5% low fat milk (in PBS-T containing 137 mM NaCl, 2.7 mM KCl, 4.3 mM $Na_2HPO_4$ 1.4 mM $KH_2PO_4$, 0.1% Tween 20, pH 7.4), the membranes were cut into sections containing different target proteins and incubated with primary antibodies against $Ca_v\alpha_2\delta_1$ (mouse, 1:1000, catalog #D219, Sigma), TSP4 (rabbit, 1:1000, custom made and validated against purified TSP4 proteins, Genscript, Piscataway, NJ), $\beta$-actin (mouse, 1:10,000, catalog #MAB8929, validated against various $\beta$-actin expressing cell lines, Novus Biologicals, LLC, Littleton, CO) overnight at 4 °C followed by horseradish peroxidase-conjugated secondary antibody (1:2000, Cell Signaling, Danvers, MA) for 1 h at room temperature. After a brief incubation with chemiluminescent reagents (Thermo Scientific, Waltham, MA), the band densities were quantified by either imaging quantification (Kodak Image Station 2000MM) or densitometry within the linear range of the film sensitivity curve. The $Ca_v\alpha_2\delta_1$ band detected by the mouse $Ca_v\alpha_2\delta_1$ antibodies reflected the $Ca_v\alpha_2$ protein only (≈150 kDa) as the $Ca_v\delta_1$ peptide separates from the $Ca_v\alpha_2$ protein under reducing conditions in Western blots (55). For quantification, band density ratios for the protein of interest over that of $\beta$-actin (≈42 kDa) were calculated within each sample first for normalization of total protein loading before cross-sample comparisons. Band density variations for the proteins of interest in the contralateral (non-injury) side were determined by comparing each band density with the mean of that from at least two different control samples in the same Western blot after taking the ratios to $\beta$-actin band densities.

### *Spinal Cord Slice Recording*

$\alpha$-Amino-3-hydroxyl-5-methylisoxazole-4-propionic acid (AMPA) receptor-mediated mEPSC and evoked excitatory post-synaptic currents (eEPSC) were recorded from lumbar spinal cord transverse slices (300 $\mu$m). Briefly, spinal cord slices were prepared and transferred to the recording chamber as described previously (30, 33). The patch electrode had a resistance of 5–7 megaohms when filled with pipette solution that contained 135 mM potassium gluconate, 5 mM KCl, 5 mM EGTA, 0.5 mM $CaCl_2$, 10 mM HEPES, 2 mM MgATP, and 0.1 mM GTP, pH 7.2, with an osmolarity 300 mosmol/liter. Superficial dorsal horn neurons were visualized with an upright microscope (Eclipse FN1, Nikon, Japan) and near-infrared illumination based on the gelatinous (semi-transparent) appearance of lamina II (substantia gelatinosa). Although neurons in superficial dorsal horn (including lamina I, lamina II outer or $II_o$, and lamina II inner or $II_i$) are heterogeneous (56, 57), the boundaries of laminae I, $II_o$, and $II_i$ are ambiguous in live spinal cord slices so it was difficult to classify lamina-specific neuron populations, a limitation of our sampling method. Thus, we pooled all recording data together for a general view of TSP4 effects in modulating synaptic transmission and regulation in superficial dorsal horn neurons. All recordings were performed at 32 ± 0.5 °C with MultiClamp 700B amplifiers (Axon Instruments, Molecular Devices, Union City, CA), Digidata 1440 analog-to-digital converters (Axon Instruments), and pClamp 10.2 software (Axon Instruments).

mEPSCs were recorded as described previously (2, 30, 33) in the presence of tetrodotoxin (TTX, 1 $\mu$M), strychnine (1 $\mu$M), bicuculline (10 $\mu$M), and 2-amino-5-phosphonopentanoic acid (AP5, 50 $\mu$M) to block TTX-sensitive $Na^+$, glycinergic, GABAergic, and *N*-methyl-D-aspartate (NMDA) currents, respectively. Membrane potential was held at −60 mV so that *N*-methyl-D-aspartate receptor-mediated currents were blocked (58), which only represented <10% mEPSCs in dorsal horn neurons, and the remaining 90% mEPSCs could be blocked by AMPA receptor antagonist 6-cyano-7-nitroquinoxaline-2,3-dione (CNQX) (59). Series resistance was monitored without compensation throughout the experiment (Multiclamp 700B). Cells were excluded from analysis if the series resistance changed by >20% during the whole-cell recording. Signals were analyzed using clampfit 10.3 (Molecular Devices) after the traces were low-pass-filtered at 2 kHz. Cumulative distribution of mEPSC frequency or amplitude of individual neurons from each experimental group was analyzed with Kolmogorov-Smirnov test.

eEPSCs were similarly recorded from superficial dorsal horn neurons of L4 lumbar spinal cord slices upon stimulating (0.1 ms, 0.05 Hz) the attached dorsal roots or dorsal root entry zone with 0–500-$\mu$A stimulus intensity. At least six eEPSC events were recorded at each stimulus intensity. QX314 (5 mM) was added in intrapipette solution to prevent sodium channel activation.

### *Immunohistochemistry (2, 28)*

Lumbar spinal cord and DRG samples were fixed in 4% paraformaldehyde overnight, cryoprotected in 30% sucrose, mounted in Optimum Cutting Temperature (O.C.T., Sakura Finetek, Torrance, CA), and sectioned with a cryostat (CM1900, Leica Microsystems, Wetzlar, Germany) into 10-$\mu$m slices. Slices of spinal cord samples were pretreated with heat-based antigen retrieval (10 nM sodium citrate, 0.05% Tween 20, pH 6.0, 5 min in a pressure cooker). Spinal cord and DRG slices were incubated with primary antibodies against $Ca_v\alpha_2\delta_1$ (rabbit polyclonal, custom made by Thermo Fisher Scientific Inc., Waltham, MA, for spinal cord samples after antigen retrieval; or mouse monoclonal, Sigma, for DRG samples without antigen retrieval; both antibodies were validated with $Ca_v\alpha_2\delta_1$ knock-out mice shown in Fig. 4, *A–D*), $VGlut_2$ (guinea pig, catalog #135404, validated previously (Refs. 28 and 60–62); Synaptic Systems, Germany), and PSD95 (rabbit, catalog #MA1-045, validated previously (Refs. 28, 63, and 64), Thermo Fisher Scientific) followed by secondary antibodies with Alexafluor 488 or 594 (Invitrogen) against IgG of corresponding species of the primary antibodies. Sample sections from control and experimental groups (sides) within the same set of experiments were stained at the same time. Samples were mounted with Vectashield containing DAPI for cell nuclei staining (Vector Laboratories, Burlingame, CA). Two images were taken from each superficial dorsal horn section randomly using a Zeiss LSM780 confocal microscope (UC Irvine Optical Biology Core) in 0.3-$\mu$m Z-stacks, and three consecutive Z stacks with the best signal were merged and used for data analysis with Voloc-

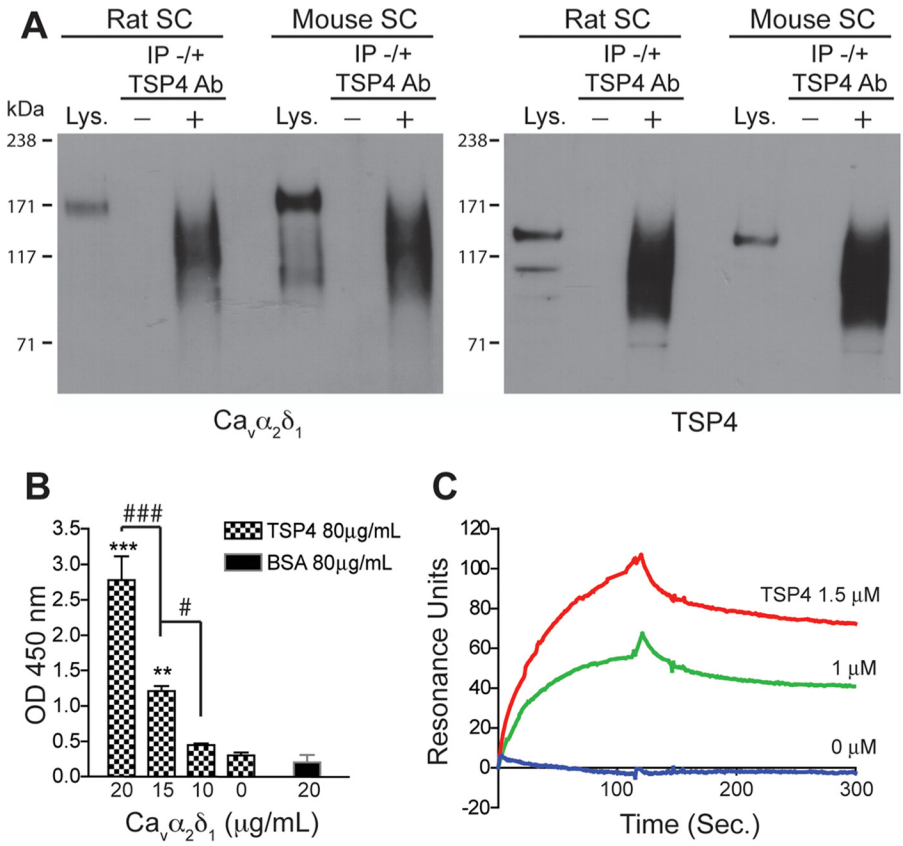


FIGURE 1. **TSP4 and $Ca_v\alpha_2\delta_1$ interaction.** Immunoprecipitation, solid-phase binding, and surface plasmon resonance binding were performed as described under "Materials and Methods" to detect TSP4/$Ca_v\alpha_2\delta_1$ interaction in rodent spinal cord and *in vitro*. *A*, typical Western blots showing $Ca_v\alpha_2\delta_1$ co-immunoprecipitation with TSP4 proteins (IP) by anti-TSP4 antibodies from rat or mouse spinal cord (*SC*) samples (from $n \geq 3$ each). *Lys*, spinal cord lysate positive control. −, no anti-TSP4 IP antibody. +, with anti-TSP4 IP antibody. Approximate positions of prestained molecular weight markers are shown on the *left of each gel*. *B*, solid phase binding showing dose-dependent FLAG-$Ca_v\alpha_2\delta_1$ binding to immobilized TSP4. **, $p < 0.01$; ***, $p < 0.001$ compared with no $Ca_v\alpha_2\delta_1$; #, $p < 0.05$; ###, $p < 0.001$ between adjacent doses by one-way ANOVA with Bonferroni post-tests. *C*, surface plasmon resonance binding sensogram of dose-dependent TSP4 binding to captured $Ca_v\alpha_2\delta_1$ (typical of three independent experiments).

ity 6.0 (PerkinElmer Life Sciences). Briefly, images from control and experimental groups within the same set of experiment were captured with the same setting. Volocity Find Object Using Percentage Intensity function was used to define background threshold, which was used for both contralateral and injury sides within each set of experiment. Fluorescent immunoreactivities above the background level were selected for analysis. From TSP4 or saline-injected mouse samples, $VGlut_2$/PSD95 co-stained samples ($n = 36$ over 3 animals, 100 $\mu$m apart) were analyzed to determine the numbers of total $VGlut_2^+$ (green), $PSD95^+$ (red), and $VGlut_2^+/PSD95^+$ (yellow) puncta. Because the effect of intrathecal injection was bilateral, the ratio of $VGlut_2^+/PSD95^+$ over $VGlut_2^+/PSD95^-$ puncta from both sides was used to compare the differences between the TSP4- and saline-treated groups. From 2-week SNL samples, $VGlut_2/Ca_v\alpha_2\delta_1$ ($n = 60$ over 3 animals, 100 $\mu$m apart) co-stained samples were analyzed to determine the numbers of total $Ca_v\alpha_2\delta_1$ (red), $VGlut_2^+$ (green), and $VGlut_2^+/Ca_v\alpha_2\delta_1^+$ (yellow) puncta. Data from the injury (ipsilateral) side were compared with that from the non-injury (contralateral) side.

### *Statistics*

One-way or two-way ANOVA with post-tests were performed for multigroup comparisons, and unpaired Student's *t* tests were performed for pair-wise comparisons as indicated in figure legends. Significance was determined by a two-tailed *p* value $< 0.05$.

## Results

*TSP4 Interacts Directly with $Ca_v\alpha_2\delta_1$ in Rodent Spinal Cord in Vivo*—Data from *in vitro* immunoprecipitation and functional assays suggest that TSP4/$Ca_v\alpha_2\delta_1$ forms a complex in mediating abnormal excitatory synapse formation in rat cerebral cortex (8). However, a direct binding or functional interaction between these proteins in spinal cord has not been shown. If interactions of these proteins lead to abnormal synaptogenesis and neuropathic pain states post injury, there should be direct molecular interactions between astrocyte-secreted TSP4 and $Ca_v\alpha_2\delta_1$ in the adult spinal cord *in vivo*. To test this, we first examined if TSP4 and $Ca_v\alpha_2\delta_1$ proteins were detectable in immunoprecipitation (IP) complexes from rodent spinal cord samples. Our results confirmed previous findings in rat cerebral cortex (8) and showed that $Ca_v\alpha_2\delta_1$ was detectable in TSP4 immunoprecipitates from rat and mouse spinal cord (Fig. 1*A*), suggesting that these proteins may interact directly or indirectly in rodent spinal cord. The differences in the patterns of bands between the spinal cord lysates and IP samples are likely due to these factors. First, IP samples were more concentrated compared with the "Lys" control samples as we loaded an equal volume of each sample onto the same blot. Under non-reducing

conditions, the IP complexes might contain more target proteins and other associated proteins. Second, it is possible, but needs to be confirmed, that TSP4 antibodies might have pulled down the extracellular $Ca_v\alpha_2$ domain (150 kDa) of the $Ca_v\alpha_2\delta_1$ subunit (175 kDa) without the $Ca_v\delta_1$ peptide (25 kDa).

To further assess whether TSP4 interacts with $Ca_v\alpha_2\delta_1$ directly, we examined interactions with solid phase binding and surface plasmon resonance spectroscopy assays. The solid phase binding assay confirmed that recombinant $Ca_v\alpha_2\delta_1$ proteins bind directly to immobilized TSP4 in a dose-dependent fashion (Fig. 1*B*). Conversely, surface plasmon resonance spectroscopy demonstrated dose-dependent binding of TSP4 to immobilized $Ca_v\alpha_2\delta_1$ on a BIAcore CM5 sensor chip with fast association and slow dissociation (Fig. 1*C*).

*Interdependent Interactions between TSP4 and $Ca_v\alpha_2\delta_1$ Proteins Contribute to Pain States and Dorsal Horn Neuron Sensitization*—If TSP4 induces neuropathic pain by interacting with $Ca_v\alpha_2\delta_1$, then blocking this interaction pharmacologically should abrogate TSP4-induced pain. It is known that gabapentin specifically binds to $Ca_v\alpha_2\delta_1$ (17, 18) and blocks neuropathic pain states induced by nerve injury-induced $Ca_v\alpha_2\delta_1$ (23–25). Thus, we tested whether gabapentin treatment could reverse TSP4-induced pain states. As reported previously (2), TSP4 intrathecal (i.t.) injection (45 $\mu$g/rat) induced tactile allodynia as evidenced by reduced PWT to von Frey filament (mechanical) stimulation 3 days post-TSP4 injection (*open bars*, Fig. 2*A*). One hour after gabapentin injection (300 $\mu$g/rat, i.t.), PWT increased to near the control levels. The effect of gabapentin was reversible because PWT were again reduced to the pretreatment level 24 h post-gabapentin treatment (*filled bars*, Fig. 2*A*). Gabapentin treatment had a similar effect on TSP4-induced thermal hyperalgesia and mechanical hyperalgesia (data not shown).

We previously reported that TSP4-induced pain states correlated with increased mEPSC frequency, but not amplitude, in superficial dorsal horn neurons (2). If TSP4 mediates this effect via ongoing interaction with $Ca_v\alpha_2\delta_1$, then blocking $Ca_v\alpha_2\delta_1$ with gabapentin should reduce mEPSC frequency. Consistent with our previous study (2), recordings from superficial dorsal horn neurons 3 days after TSP4 injection revealed a significant >100% increase in average mEPSC frequency without significant changes in its amplitude (Fig. 2, *B1*, *B2*, and *B3*). After treatment with gabapentin (50 $\mu$M), elevated mEPSC frequency was dramatically decreased to the control level, but its basal level in the control group was not affected significantly (Fig. 2, *B1* and *B4*). These changes were confirmed by Kolmogorov-Smirnov tests using cumulative distribution of mEPSC frequency or amplitude of individual neurons from each experimental group (*bottom panels* of Fig. 2, *B2–B4*). This gabapentin concentration is close to that in patient cerebrospinal fluid after chronic gabapentin treatments. It has been reported that oral 900 mg/day gabapentin treatment for 3 months can reach peak plasmid concentration ~10 mg/liter (58 $\mu$M) 3 h after the last dose (65), and cerebrospinal fluid gabapentin concentration range was ~20–35% that in the plasma after multiple dosing (65, 66). Collectively, these results support the idea that TSP4/$Ca_v\alpha_2\delta_1$-dependent processes mediate both TSP4-induced pain states and the putative pathological underpinning (increased mEPSC frequency).

To further test whether blocking TSP4/$Ca_v\alpha_2\delta_1$-dependent processes by biochemical knocking down $Ca_v\alpha_2\delta_1$ could prevent TSP4-induced pain states, we investigated if TSP4-induced behavioral hypersensitivity could be prevented by preemptive knockdown of $Ca_v\alpha_2\delta_1$ with intrathecal treatment of anti-$Ca_v\alpha_2\delta_1$ small hairpin RNA in AAV vectors ($Ca_v\alpha_2\delta_1$-AAV). We previously showed that bolus intrathecal TSP4 injection induced tactile allodynia as evidenced by progressive reduction in PWT to a tactile stimulus (2). This effect was confirmed in the present study in rats that were pretreated with intrathecal control AAV ($10^6$ units in 2 $\mu$l) 10 days before bolus TSP4 injection (45 $\mu$g/rat, i.t.) (Fig. 2*C*). In contrast, rats pretreated with $Ca_v\alpha_2\delta_1$-AAV ($10^6$ units in 2 $\mu$l), which diminished dorsal spinal cord $Ca_v\alpha_2\delta_1$ levels (Fig. 2*C*, *inset*), did not exhibit the progressive decreases in PWT that reflect tactile allodynia (Fig. 2*C*). These results support the conclusion that TSP4-induced allodynia does depend on $Ca_v\alpha_2\delta_1$.

To further test this idea in the clinically relevant neuropathic model of SNL, we investigated whether knock down of $Ca_v\alpha_2\delta_1$ by intrathecal $Ca_v\alpha_2\delta_1$-AAV could reverse SNL-induced behavioral hypersensitivity as our previous studies have implicated either $Ca_v\alpha_2\delta_1$ or TSP4 in neuropathic pain states (2, 24, 25, 28, 29). Bolus i.t $Ca_v\alpha_2\delta_1$-AAV, but not the control vector, treatments ($10^6$ units in 2 $\mu$l) caused a time-dependent reversal of 2-week SNL-induced tactile allodynia without affecting the behavioral sensitivity in the contralateral (non-injury) side. The anti-allodynic effects of $Ca_v\alpha_2\delta_1$-AAV peaked ~10 days after the i.t. injection (Fig. 2*D1*) and lasted for >2 weeks (data not shown). Western blot analysis of spinal cord samples from control and $Ca_v\alpha_2\delta_1$-AAV-treated rats at the peak allodynia reversal time point (10 days post-$Ca_v\alpha_2\delta_1$-AAV treatment) confirmed $Ca_v\alpha_2\delta_1$ knockdown on both sides of dorsal spinal cord. $Ca_v\alpha_2\delta_1$ levels on the injury side were not significantly different from levels in the non-injury side of control vector-treated rats (Fig. 2*D2*). The fact that $Ca_v\alpha_2\delta_1$ knockdown prevented allodynia development (Fig. 2*C*) and reversed established allodynia (Fig. 2*D1*) indicates that TSP-induced behavioral hypersensitivity requires ongoing interactions between TSP4 and $Ca_v\alpha_2\delta_1$ at the spinal cord level.

Next, we examined if blocking TSP4 could diminish pain states and putative pathological underpinning due to elevation of $Ca_v\alpha_2\delta_1$. We previously showed that TG mice with neuronal $Ca_v\alpha_2\delta_1$ overexpression have increased mEPSC frequency and pain states similar to mice with SNL injury (30, 33, 34, 59, 67). We first tested whether blocking TSP4-dependent processes with TSP4 antibodies would reverse $Ca_v\alpha_2\delta_1$ overexpression-induced allodynia. Consistent with previous findings (34), TG mice with neuronal $Ca_v\alpha_2\delta_1$ overexpression have greatly reduced PWT to mechanical stimuli (the behavioral reflection of allodynia). After treatment with the TSP4 antibody (10 $\mu$g/mouse, i.t., chicken polyclonal, validated previously; Ref. 68), PWT gradually increased to near the control level by 8 h post-treatment and then returned to the pretreatment level by 24 h (Fig. 3*A1*). Antibody treatment did not affect baseline thresholds in age- and sex-matched wild type (WT) mice. Heat-denatured antibody was without effect (Fig. 3*A1*). Similar treat-

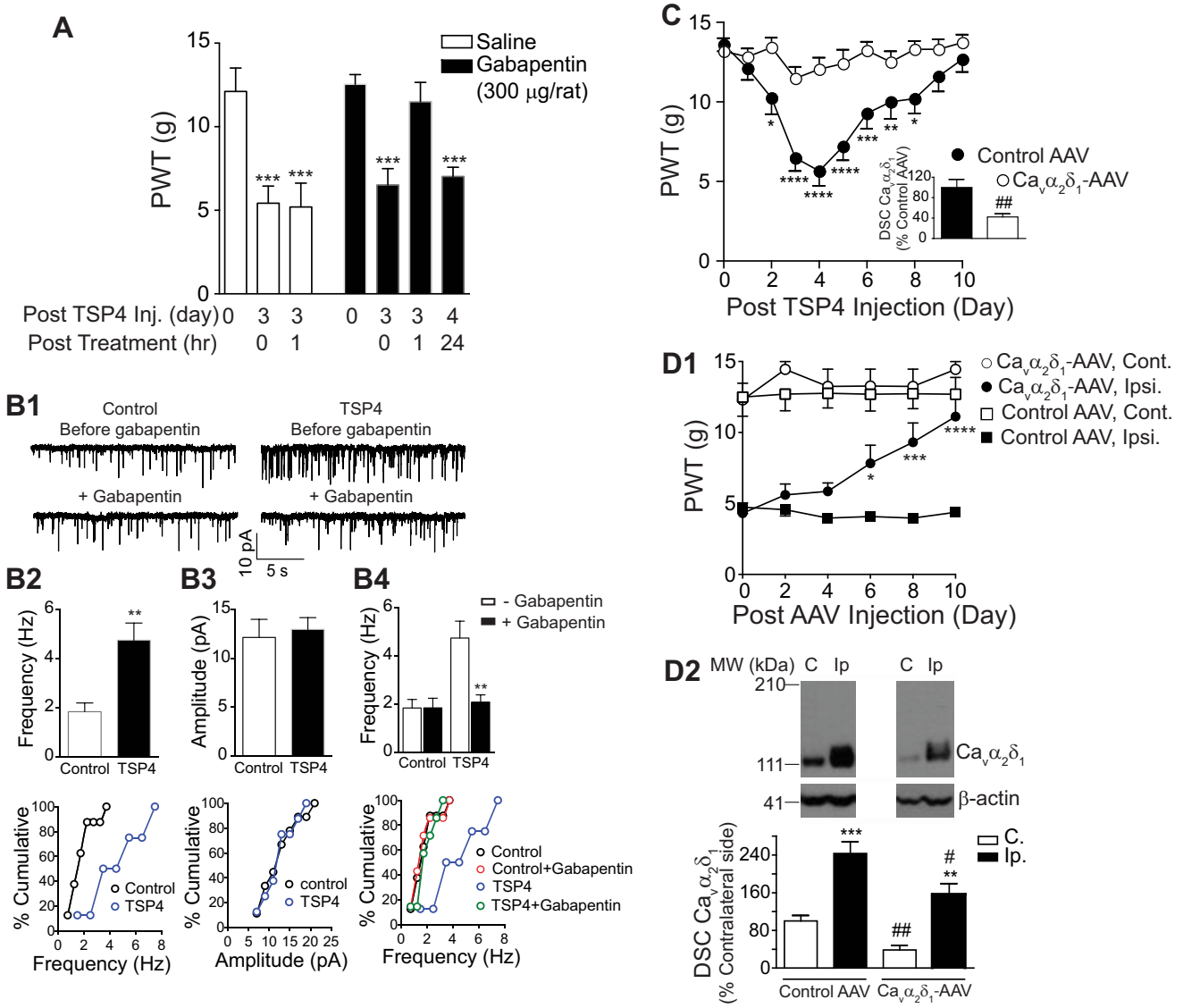


FIGURE 2. **Blocking or depleting Ca$_v$α$_2$δ$_1$ reverses pain states and exaggerated presynaptic excitatory input induced by elevated TSP4 or SNL.** *A*, Gabapentin (i.t. injected 3 days post-TSP4 injection) reversed tactile allodynia induced by TSP4 (45 μg/rat, i.t.) in 1 h. Data are the means ± S.E. from $n = 6$ (saline) to 8 (gabapentin (*GBP*)) rats. ***, $p < 0.001$ *versus* pre-TSP4 by one-way ANOVA with Bonferroni post-tests. *B1*, mEPSCs from rat L5 superficial dorsal horn neurons 3 days after the same TSP4 injection. *Top*, mEPSC frequency, but not amplitude, was increased in TSP4 injected rats *versus* control rats injected with an equal molar dose of His-tag peptides. *Bottom*, gabapentin (50 μM) blocked the TSP4 effects. *B2–B4*, *top*, summarized data. Date are the means ± S.E., $n \geq 7$ neurons from 4 rats in each group. **, $p < 0.01$ compared with control (*B2*) or pre-treatment (*B4*) level by Student's *t* test. *B2–B4 bottom*, cumulative distribution of mEPSC frequency (*B2 bottom*) and amplitude (*B3 bottom*) in neurons from control and TSP4 injected rats ($p < 0.01$ for comparison of mEPSC frequency; $p > 0.05$ for comparison of mEPSC amplitude; Kolmogorov-Smirnov test). *B4 bottom*, application of gabapentin (50 μM) significantly reduced the mEPSCs frequency in neurons from TSP4-injected rats to a level similar to that in control neurons ($p < 0.001$ for comparison of mEPSC frequency before and during gabapentin treatment in TSP4 injected group; Kolmogorov-Smirnov test). *C*, preemptive knockdown of Ca$_v$α$_2$δ$_1$ in rat dorsal spinal cord (*DSC*, *inset*) with bolus intrathecal injection (L5/6 region) of anti-Ca$_v$α$_2$δ$_1$ small hairpin RNA (*Ca$_v$α$_2$δ$_1$-AAV*), but not control (*Control-AAV*), AAV vectors ($10^6$ units in 2 μl) 10 days before TSP4 injection (45 μg/10 μl/rat, i.t. at day 0) blocked TSP4-induced allodynia. Data are the means ± S.E. from seven rats each. *, $p < 0.05$; **, $p < 0.01$; ***, $p < 0.001$; ****, $p < 0.0001$ *versus* pre-TSP4 by repeated measures two-way ANOVA analysis with Bonferroni post-tests; ##, $p < 0.01$ *versus* the control AAV group by Student's *t* test (*inset*). *D1*, similar intrathecal injection of Ca$_v$α$_2$δ$_1$, but not control, AAV into L5/6 regions of 2-week SNL rats led to a gradual reversal of established allodynia in the hind paws of the injury (*Ipsi.*) side without affecting the behavioral sensitivity in that of the non-injury (*Cont.*) side. Data are the means ± S.E. from six rats each. *, $p < 0.05$; ***, $p < 0.001$; ****, $p < 0.0001$ compared with the pretreatment level by repeated measures two-way ANOVA analysis with Bonferroni post-tests. *D2*, dorsal spinal cord Ca$_v$α$_2$δ$_1$ levels were down-regulated significantly from both sides of rats similarly injected with Ca$_v$α$_2$δ$_1$-AAV 10 days ago compared with that in rats injected with the control AAV. *Top*, representative images from the same Western blot showing Ca$_v$α$_2$δ$_1$ levels in both sides of dorsal spinal cord samples. β-Actin bands were used for normalization of total protein loading (see "Materials and Methods"). Approximate positions of prestained molecular weight (*MW*) markers are shown on the *left*. *Bottom*, summarized Western blot data. Data are the means ± S.E. from six rats each. **, $p < 0.01$; ***, $p < 0.001$ compared with non-injury side. #, $p < 0.05$; ##, $p < 0.01$ compared with the same side in control-AAV treated rats by Student's *t* test. *C*, contralateral (non-injury) side. *Ip*, ipsilateral (injury) side.

ment with this antibody also prevented the development and reversed established neuropathic pain states in the more clinically relevant SNL model (2).

As an alternative approach, we tested if genetic ablation of TSP4 from the Ca$_v$α$_2$δ$_1$ TG mice would eliminate behavioral hypersensitivities previously reported in Ca$_v$α$_2$δ$_1$ TG mice (30, 33, 34, 59). To test this, we crossed Ca$_v$α$_2$δ$_1$ TG mice that develop hypersensitivity to stimuli with TSP4 knock-out mice to generate Ca$_v$α$_2$δ$_1$ TG/TSP4 KO mice with elevated neuronal Ca$_v$α$_2$δ$_1$ and TSP4 ablation. Similar to our previous findings

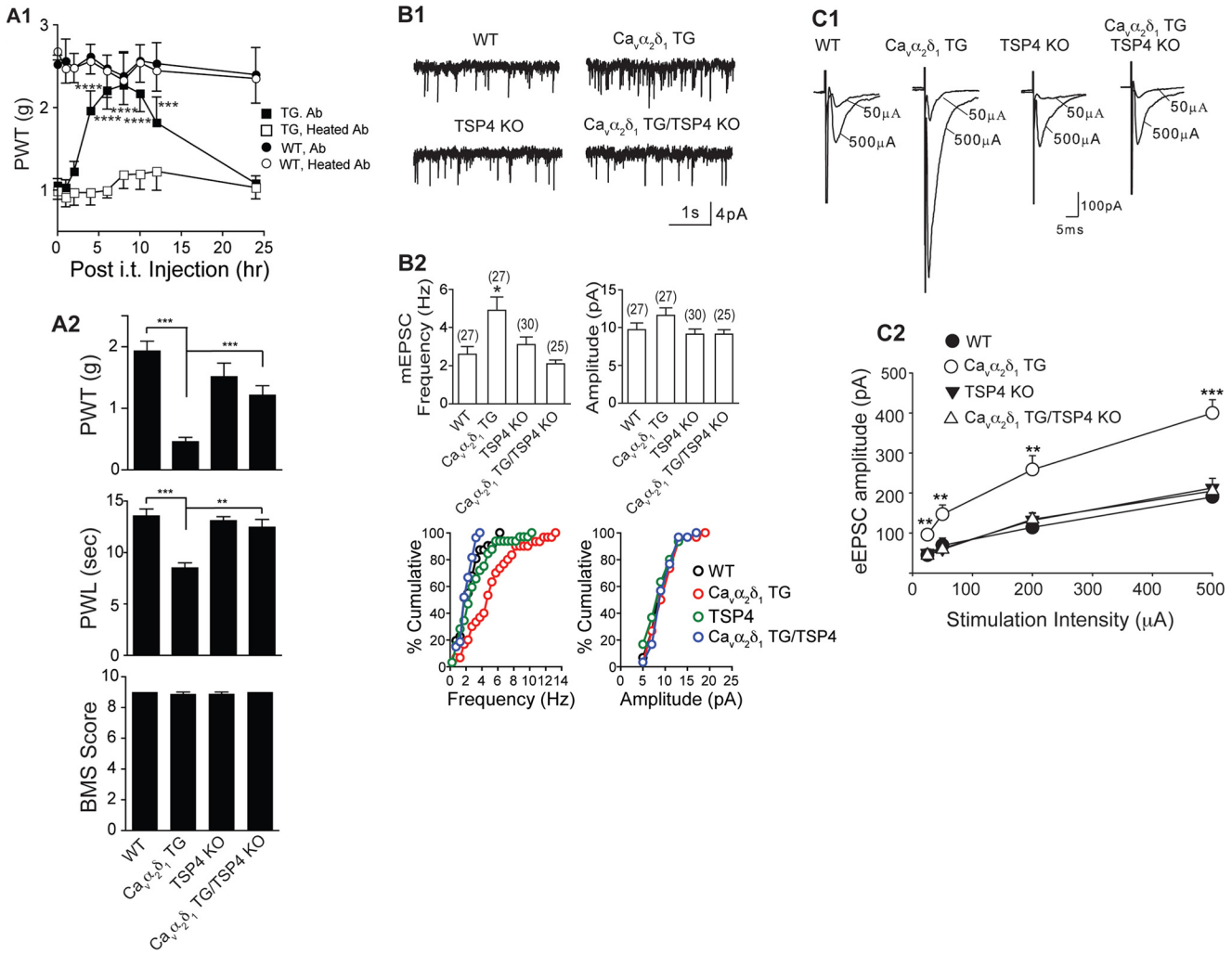


FIGURE 3. **Depleting or blocking TSP4 reverses $Ca_v\alpha_2\delta_1$-induced pain states and dorsal horn neuron sensitization.** *A1*, TSP4 antibody (*Ab*, chicken, 10 μg/5 μl/mouse, i.t.), but not heated TSP4 antibody, reversed allodynia induced by neuronal $Ca_v\alpha_2\delta_1$ overexpression in the $Ca_v\alpha_2\delta_1$-TG mice without affecting baseline sensitivity in WT mice. Data are the means ± S.E. from $n = 5$ (WT) or 6 (TG). ***, $p < 0.001$; ****, $p < 0.0001$ *versus* pretreatment level by repeated measures two-way ANOVA with Bonferroni post-tests. *A2*, TSP4 ablation did not affect baseline sensitivity but reversed tactile allodynia (*top*) and thermal hyperalgesia (*middle*) in the $Ca_v\alpha_2\delta_1$ TG mice. Locomotor functions were not affected in these genetically modified mice as analyzed with the Basso Mouse Scale for locomotion (*BMS*), *bottom*). Data are the means ± S.E. from $n = 8$–10 each group. **, $p < 0.01$; ***, $p < 0.001$ by Student's *t* test. *B1*, mEPSCs from L4 superficial dorsal horn neurons of the same mouse groups. $Ca_v\alpha_2\delta_1$-induced increase of mEPSC frequency in the $Ca_v\alpha_2\delta_1$ TG mice was blocked by TSP4 ablation. *B2 top*, summarized data. Data are the means ± S.E. from the number of neurons shown in parentheses that were obtained from ≥ 5 mice in each group. *, $p < 0.05$ *versus* WT by one-way ANOVA with Bonferroni post-tests. *B2 bottom*, cumulative distribution of mEPSC frequency and amplitude in each group ($p < 0.01$ for frequency comparisons between the $Ca_v\alpha_2\delta_1$ TG group and each of the other three groups; Kolmogorov-Smirnov test). *C1*, TSP4 ablation also blocked $Ca_v\alpha_2\delta_1$-induced increase of eEPSC amplitude in response to dorsal root entry zone stimulation without affecting baseline eEPSCs significantly. *C2*, summarized data, means ± S.E. from $n \geq 7$ for each stimulus intensity (≥5 mice). **, $p < 0.01$; ***, $p < 0.001$ *versus* WT by repeated measures two-way ANOVA with Bonferroni post-tests.

(34), $Ca_v\alpha_2\delta_1$ overexpression in the TG mice resulted in behavioral hypersensitivities to mechanical (allodynia; Fig. 3*A2*, *top*) and thermal (thermal hyperalgesia; Fig. 3*A2*, *middle*) stimuli. Assessment of pain sensitivity in $Ca_v\alpha_2\delta_1$ TG/TSP4 KO mice revealed no increased sensitivity to either of these stimuli. Behavioral thresholds in mice with TSP4 knock-out alone (TSP4 KO) were comparable with that in WT control mice (Fig. 3*A2*, *top* and *middle*). The locomotor function test scores of Basso Mouse Scale (*BMS*) in mice with these genetic modifications were similar to that in the control mice (Fig. 3*A2*, *bottom*). Thus, TSP4 basal level is not critical in maintaining basal sensory/motor functions, and differences in behavioral sensitivities to stimuli among these mouse groups are not due to changes in motor functions. Together, these findings support that TSP4/$Ca_v\alpha_2\delta_1$-dependent processes are also required for pain state processing induced by elevated $Ca_v\alpha_2\delta_1$.

We also assessed whether the increase in mEPSC frequency reported previously in $Ca_v\alpha_2\delta_1$ TG mice (30, 33, 59) could be normalized by deleting TSP4 from the $Ca_v\alpha_2\delta_1$ TG/TSP4 KO mice. Similar to our previous findings (30, 33, 59), recordings from superficial dorsal horn neurons of $Ca_v\alpha_2\delta_1$ TG mice revealed significantly elevated frequency, but not amplitude, of mEPSC compared with that from control WT mice (Fig. 3*B*). As another control, recordings from superficial dorsal horn neurons of TSP4 KO mice revealed mEPSC frequency/amplitude comparable with that seen in WT neurons (Fig. 3*B*). However, recordings from superficial dorsal horn neurons of $Ca_v\alpha_2\delta_1$ TG/TSP4 KO mice revealed that mEPSC frequency and ampli-

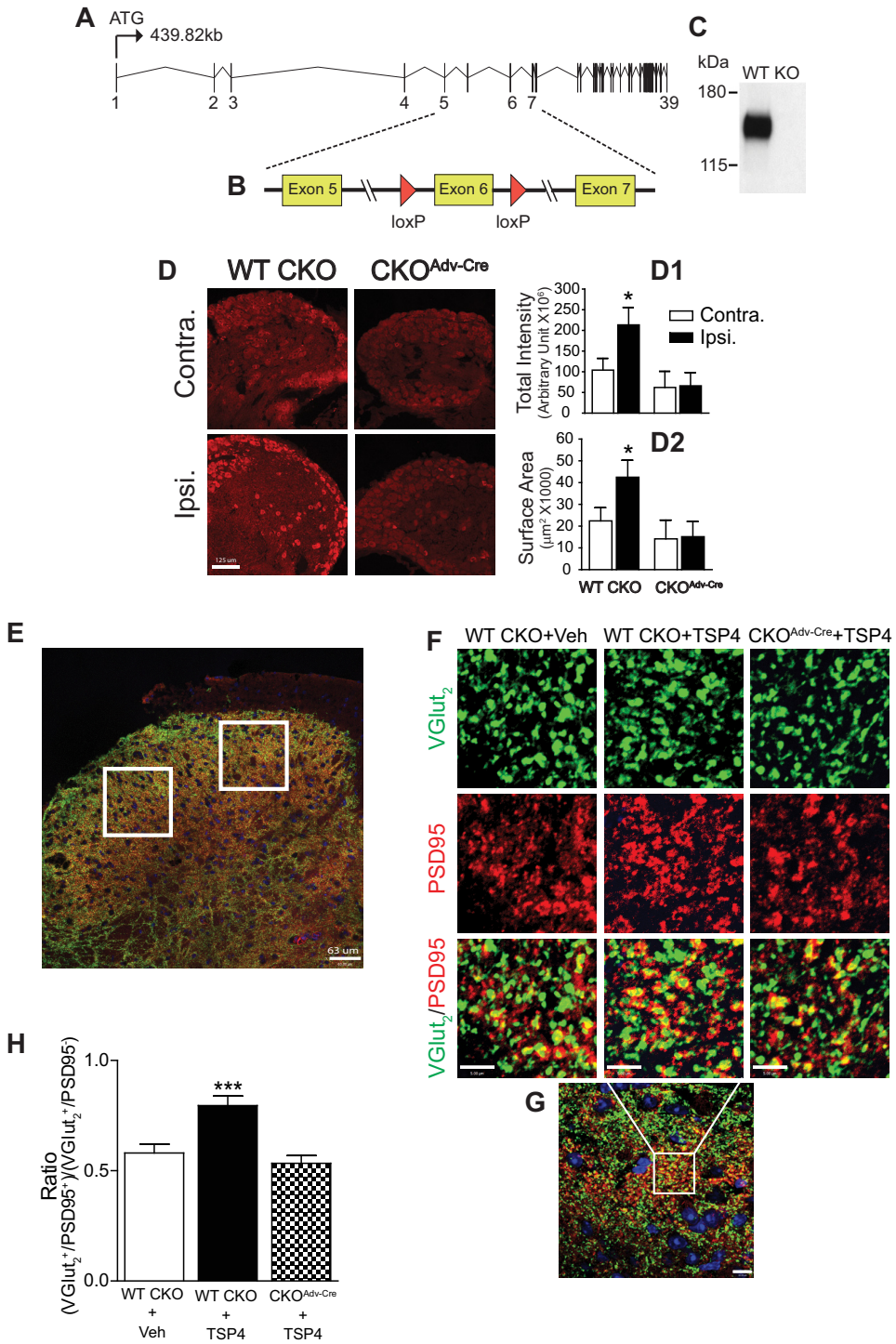


FIGURE 4. **$Ca_v\alpha_2\delta_1$ ablation from Advillin$^+$ DRG neurons blocked TSP4-induced excitatory synaptogenesis.** *A*, $Ca_v\alpha_2\delta_1$ gene structure. *B*, a strategy diagram of generating the $Ca_v\alpha_2\delta_1$ conditional knock-out mice. *C*, a representative Western blot (from $n = 3$) showing null $Ca_v\alpha_2\delta_1$ expression (*KO*) in brain lysates from homozygous $Ca_v\alpha_2\delta_1$ KO mice crossed with germ line Cre mice (FVB/N-Tg(ACTB-cre)$^{2Mrt/J}$ (The Jackson Laboratory). *D*, validation of $Ca_v\alpha_2\delta_1$ conditional knock-out from Advillin-Cre expressing DRG neurons in 2-week SNL WT CKO control or CKO$^{Adv\text{-}Cre}$ mice with $Ca_v\alpha_2\delta_1$ antibody immunofluorescent staining (*red*). *Contra.*, non-injury; *Ipsi.*, injury side. Summarized total intensity (*D1*) and surface area (*D2*) data are presented as the means ± S.E. from 12 sections, three mice in each group. *, $p < 0.05$ compared with non-injury (*contra.*) side in each group with paired Student's *t* test. *Scale bar*: 125 μm for all panels. *E*, a representative L4 dorsal spinal cord image showing random sampling (*white squares*) of fluorescent immunoreactivity from superficial dorsal horn for data analysis. *Scale bar*: 63 μm. *F*, representative images from co-immunostaining in thin sections of L4 dorsal spinal cord from WT CKO or CKO$^{Adv\text{-}Cre}$ mice 4-days post-i.t. saline (vehicle) or TSP4 (5 μg/5 μl/mouse) injection. $VGlut_2$ (*green*), excitatory presynaptic marker; PSD95 (*red*), post-synaptic marker; *yellow*, colocalized immunoreactivity. *Scale bar*: 5 μm for all panels. Each of these images was enlarged to show detailed structure from a small area (similar to the *white box in G*) of a sampling image. *G*, a representative sampling image showing the area (in the *white box*) that was enlarged to show detailed structure above. *Scale bar*: 10 μm. *H*, summarized ratio of $VGlut_2^+/PSD95^+$ over $VGlut_2^+/PSD95^-$ immunoreactive puncta. Data are the means ± S.E., 36 sections from 3 mice each. ***, $p < 0.001$ *versus* vehicle injected WT CKO mice by one-way ANOVA with Dunnett's post hoc test.

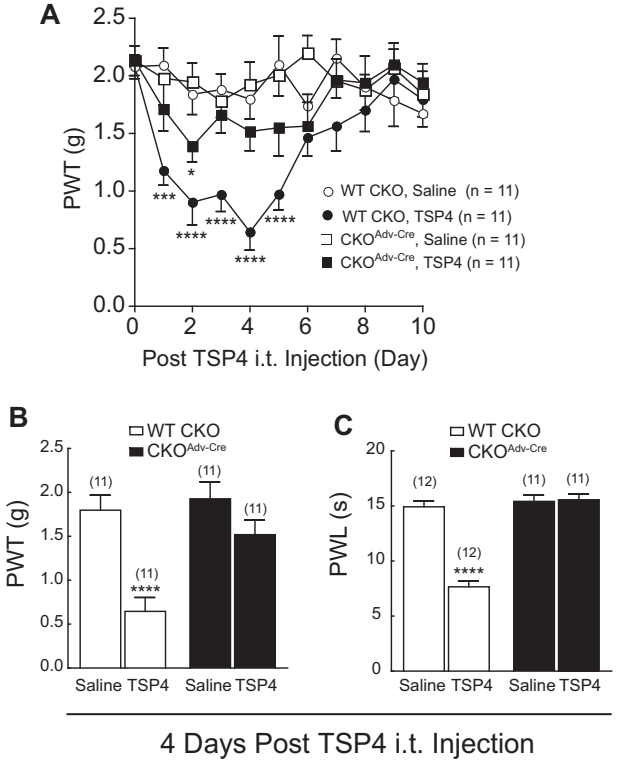


FIGURE 5. **$Ca_v\alpha_2\delta_1$ ablation from DRG neurons blocked TSP4-induced pain states.** Hind paw sensitivities to mechanical and thermal stimuli were measured in control WT CKO or $CKO^{Adv\text{-}Cre}$ mice post-bolus TSP4 (5 $\mu$g/5 $\mu$l/mouse, i.t.) injection as described under "Materials and Methods." *A*, time course of TSP4-induced tactile allodynia in WT CKO mice that was diminished in $CKO^{Adv\text{-}Cre}$ mice with $Ca_v\alpha_2\delta_1$ ablation from Advillin$^+$ DRG neurons. Data are the means ± S.E. *, $p < 0.05$; ***, $p < 0.001$; ****, $p < 0.0001$ *versus* pre-treatment level by repeated measures two-way ANOVA with Bonferroni post-tests. Peak allodynia (*B*) and thermal hyperalgesia (*C*) seen in WT CKO mice were blocked in $CKO^{Adv\text{-}Cre}$ mice. Data are the means ± S.E. from (*n*) indicated. ****, $p < 0.0001$ *versus* saline group by Student's *t* test.

tude were within the range of that in control mice (Fig. 3*B*). These findings were confirmed by Kolmogorov-Smirnov tests using cumulative distribution of mEPSC frequency or amplitude of individual neurons from each experimental group (*bottom panels* of Fig. 3*B2*). Collectively, these findings support that although basal level TSP4 is not required for maintaining a normal level of mEPSC, TSP4/$Ca_v\alpha_2\delta_1$-dependent processes are required for $Ca_v\alpha_2\delta_1$-induced increase of mEPSC frequency, an indication of enhanced presynaptic excitatory input.

We hypothesized that increased TSP4/$Ca_v\alpha_2\delta_1$ interactions in the spinal cord of the TG mice could lead to hyperexcitability of dorsal horn neurons to peripheral stimulation. To test this, we examined the amplitude of eEPSCs in L4 superficial dorsal horn neurons from the $Ca_v\alpha_2\delta_1$ TG mice in response to escalating intensities of stimulation to dorsal root entry zone. Compared with that from WT littermates, eEPSC amplitudes were increased at all levels of stimulus intensity tested (Fig. 3*C*), indicating hyperresponsiveness of the dorsal horn neurons to afferent activation as a result of $Ca_v\alpha_2\delta_1$ overexpression. Similar recordings in $Ca_v\alpha_2\delta_1$ TG/TSP4 KO mice revealed that eEPSC frequency was within the range of WT mice, as was also the case with TSP4 KO alone (Fig. 3*C*). These findings suggest that although basal level TSP4 is not required for maintaining normal dorsal horn neuron excitatory tone, TSP4/$Ca_v\alpha_2\delta_1$-dependent processes are required for $Ca_v\alpha_2\delta_1$-mediated dorsal horn neuron sensitization.

*Interdependent Interactions between TSP4 and $Ca_v\alpha_2\delta_1$ Proteins Promote Aberrant Excitatory Synaptogenesis in Animal Models with Pain States*—Previous studies have shown that $Ca_v\alpha_2\delta_1$ proteins in sensory neurons are transported to central afferent terminals in the spinal dorsal horn under normal and post-injury conditions (27, 29). Other studies have shown that TSP interactions with $Ca_v\alpha_2\delta_1$ promote excitatory synaptogenesis *in vitro* (8) and increased excitatory synapses are associated with neuropathic pain states (28, 69). Together, these findings raise the possibility that injury-induced TSP4 in spinal cord might interact with $Ca_v\alpha_2\delta_1$ at the pre-synaptic terminals of sensory afferents to promote aberrant excitatory synaptogenesis, which in turn would contribute to enhanced transmission along pain pathways.

To test this hypothesis, we took the first step in determining whether there was evidence for aberrant excitatory synaptogenesis with TSP4-induced pain states; when so, we tried to determine if genetic ablation of $Ca_v\alpha_2\delta_1$ could block TSP4-induced synaptogenesis. We generated $Ca_v\alpha_2\delta_1$ conditional knock-out (WT CKO) mice in which exon 6 of the $Ca_v\alpha_2\delta_1$ gene was floxed with loxP sites (Fig. 4, *A* and *B*). Crossing these mice with Cre-recombinase expressing mice resulted in deletion of $Ca_v\alpha_2\delta_1$ from Cre-expressing cells (Fig. 4*C*). The WT CKO mice were crossed with Advillin-Cre mice with Cre recombinase expression only in Advillin-positive sensory neurons that cover ~94% of all DRG neurons (35). Cre-driven $Ca_v\alpha_2\delta_1$ deletion from DRG neurons in homozygous $CKO^{Adv\text{-}Cre+/-}$ mice was confirmed by immunostaining data showing that 2-week SNL could induce DRG $Ca_v\alpha_2\delta_1$ up-regulation indicated as increased $Ca_v\alpha_2\delta_1$ antibody immunoreactivity in DRG neurons of control mice (WT CKO), as we have reported previously (25), but failed to do so in homozygous $CKO^{Adv\text{-}Cre+/-}$ mice (Fig. 4*D*). We then immunostained sections of L4 lumbar spinal cord from TSP4 (5 $\mu$g/mouse, i.t.)-injected mice 4 days after the injection (peak pain states in control mice) with markers for excitatory synapses ($VGlut_2$ and post-synaptic density marker PSD95). Measurements of total number of synaptic puncta immunoreactive to both synaptic marker antibodies in spinal cord superficial dorsal horn (Fig. 4*E*) revealed substantial increases in excitatory synapses in TSP4 injected control WT CKO mice compared with vehicle-injected WT CKO mice. These TSP4-induced changes were not seen with $Ca_v\alpha_2\delta_1$ ablation in the $CKO^{Adv\text{-}Cre+/-}$ mice (Fig. 4, *F–H*). Thus, TSP4-induced aberrant excitatory synaptogenesis in dorsal spinal cord requires TSP4/$Ca_v\alpha_2\delta_1$-dependent processes.

If TSP4-induced aberrant excitatory synaptogenesis in dorsal spinal cord contributes to pain processing, one would expect to see that the absence of TSP4-induced excitatory synaptogenesis in the $CKO^{Adv\text{-}Cre+/-}$ mice correlates with the absence of TSP4-induced pain states. We tested this by examining behavioral sensitivity of control and $CKO^{Adv\text{-}Cre+/-}$ mice after TSP4 injections (5 $\mu$g/mouse, i.t.). Similar to previous findings in rats (2), TSP4 injection into control WT CKO mice led to tactile allodynia (Fig. 5, *A* and *B*) and thermal hyperalgesia (Fig. 5*C*), which peaked ~4 days after TSP4 injections that correlated

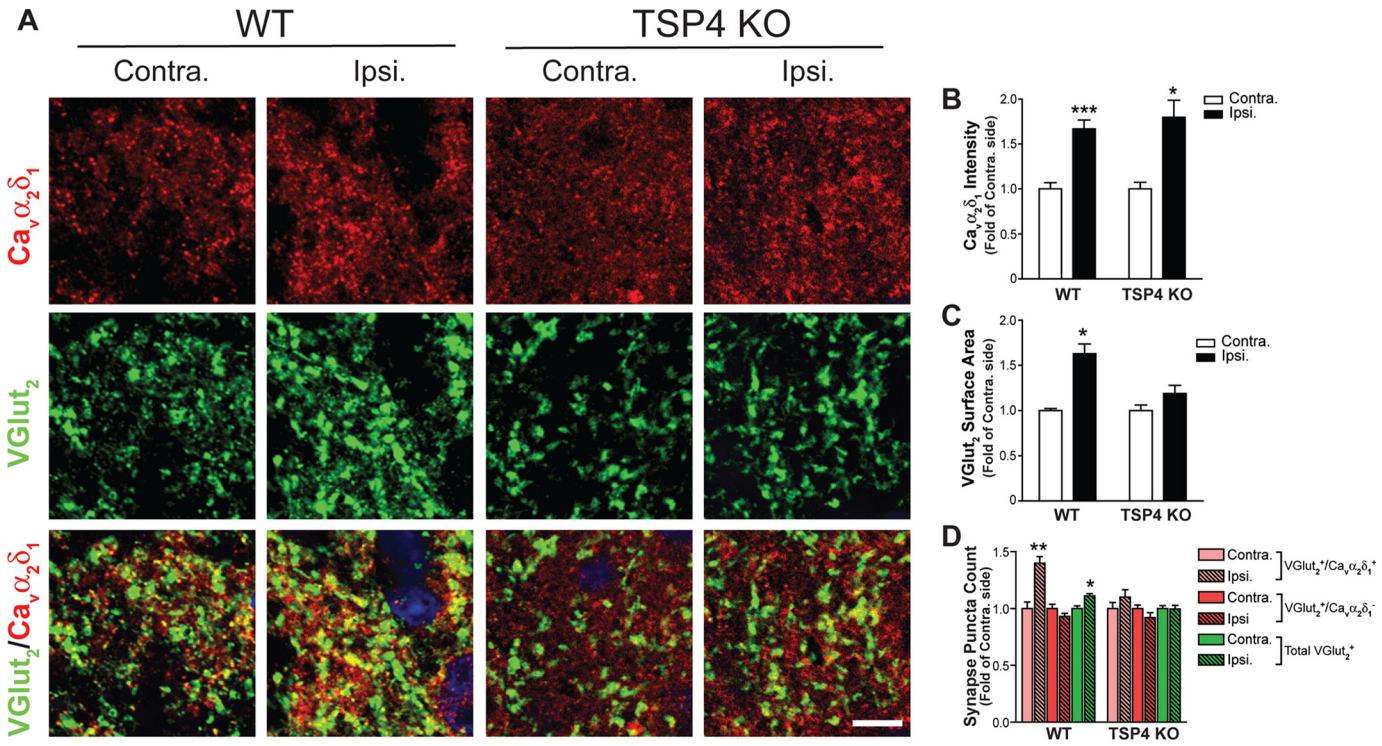


FIGURE 6. **TSP4 ablation blocked SNL-induced excitatory synaptogenesis.** Co-immunostaining of $Ca_v\alpha_2\delta_1$ with synaptic markers was performed in thin sections of dorsal spinal cord samples from two-week SNL WT or TSP4 KO mice when behavioral hypersensitivity occurred in the injury (*Ipsi.*) side of SNL WT mice but not TSP4 KO mice (2). *A*, representative images showing $Ca_v\alpha_2\delta_1$ (*red*) and $VGlut_2$ (*green*) immunoreactivity and their colocalization (*yellow*) in superficial dorsal horn. *Scale bar* = 5 $\mu$m for all image panels. Summarized data of total $Ca_v\alpha_2\delta_1$ immunoreactivity intensity (*B*), $VGlut_2$ immunoreactivity surface area (*C*), and $VGlut_2^+$ puncta with (*yellow*) or without (*green*) co-localization with $Ca_v\alpha_2\delta_1$ immunoreactivity (*D*) are presented as the means ± S.E. collected from 60 images over three mice in each group. *, $p < 0.05$; **, $p < 0.01$; ***, $p < 0.001$ compared with non-injury (*contra.*) side by paired Student's *t* test.

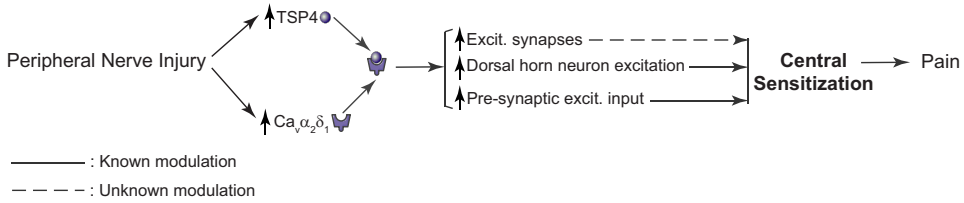


FIGURE 7. **Proposed mechanisms of the TSP4/$Ca_v\alpha_2\delta_1$ pathway in central sensitization and neuropathic pain.**

temporally with a significant increase of excitatory synapses in dorsal spinal cord of these mice (Fig. 4, *F–H*). In contrast, similar TSP4 injections into $CKO^{Adv\text{-}Cre+/-}$ mice failed to induce similar behavioral hypersensitivities (Fig. 5, *A–C*). This supports that TSP4-induced aberrant excitatory synaptogenesis through TSP4/$Ca_v\alpha_2\delta_1$-dependent processes plays a role in transmitting nociceptive signals.

We next tested whether TSP4-induced synaptogenesis also plays a role in neuropathic pain development in the more clinically relevant SNL model. Our previous study has shown that SNL-induced allodynia is diminished in SNL TSP4 KO mice (2), suggesting a role of TSP4 in mediating neuropathic pain. Immunostaining for $Ca_v\alpha_2\delta_1$ revealed increases in $Ca_v\alpha_2\delta_1$ puncta in the superficial dorsal horn of the injury side in both WT and TSP4 KO mice 2 weeks post-SNL (Fig. 6, *A* and *B*), which correlated with severe allodynia in SNL WT, but not TSP4 KO, mice (2). Thus, elevated presynaptic $Ca_v\alpha_2\delta_1$ expression is not regulated by TSP4. Nerve injury also increased $VGlut_2$ puncta that mainly co-localized with $Ca_v\alpha_2\delta_1$ puncta in the WT mice (Fig. 6, *A*, *C*, and *D*), supporting that injury-induced $Ca_v\alpha_2\delta_1$ up-regulation at the presynaptic terminals of injured afferents is associated with increased numbers of excitatory synapses in dorsal spinal card. Importantly, these changes were not seen in TSP4 KO mice with SNL (Fig. 6, *A*, *C*, and *D*). These data support that SNL does induce aberrant excitatory synaptogenesis that also requires TSP4/$Ca_v\alpha_2\delta_1$-dependent processes.

## Discussion

Peripheral nerve injury induces up-regulation of TSP4 and $Ca_v\alpha_2\delta_1$ in DRG/spinal cord that contributes to neuropathic pain states through mechanisms that were previously undefined (2, 24, 25, 27, 29, 31). Here, we provided a large body of evidence to support that TSP4/$Ca_v\alpha_2\delta_1$-dependent processes are required in promoting central sensitization and pain states.

Our data confirm that there is a direct interaction between TSP4 and $Ca_v\alpha_2\delta_1$ in rodent spinal cord and *in vitro*. In addition, blocking or down-regulating $Ca_v\alpha_2\delta_1$ can block TSP4-in-

duced pain states and increased mEPSC frequency in spinal cord neurons. Conversely, blocking or genetically deleting TSP4 can block $Ca_v\alpha_2\delta_1$ overexpression-induced behavioral hypersensitivity, increased mEPSC frequency, and exaggerated eEPSC in spinal cord neurons. Furthermore, elevated TSP4 induces an increase of spinal excitatory synapses that correlates with heightened pain states, both of which can be normalized by $Ca_v\alpha_2\delta_1$ ablation from sensory neurons. Equally, TSP4 ablation blocks injury-induced excitatory synaptogenesis associated with elevated $Ca_v\alpha_2\delta_1$ without affecting nerve injury-induced $Ca_v\alpha_2\delta_1$ up-regulation in the dorsal horn. Together, these findings support that elevated TSP4 in dorsal spinal cord can induce central sensitization by promoting exaggerated presynaptic excitatory input, excitatory synaptogenesis, and evoked excitability of dorsal horn neurons through activation of TSP4/$Ca_v\alpha_2\delta_1$-dependent processes.

In combination with previous findings from peripheral nerve injury models, our data reveal the importance of TSP4/$Ca_v\alpha_2\delta_1$-dependent processes in mediating central sensitization and chronic pain states post injury. Although TSP4 is up-regulated within days after peripheral nerve injury in both DRG and dorsal spinal cord (1, 2), there is a significant delay in peak $Ca_v\alpha_2\delta_1$ up-regulation in the dorsal horn (weeks) (29), primarily due to time required for initial translocation of elevated $Ca_v\alpha_2\delta_1$ from DRG to pre-synaptic central terminals of sensory afferents in the dorsal horn (27, 29). The subsequent interaction of elevated TSP4 with excess pre-synaptic $Ca_v\alpha_2\delta_1$ in the dorsal horn then promotes aberrant excitatory synaptogenesis and dorsal horn neuron sensitization to maintain chronic pain states (Fig. 7). Although dorsal horn neurons are heterogeneous and play distinct roles in transmitting modality-specific information (56, 57), our sampling method would not allow us to perform a sensory neuron-type-specific dissection of these changes. Further studies, for example, using Cre-directed ablation of genes of interest from subpopulations of sensory neurons is necessary to provide more deep mechanistic insights about the TSP4/$Ca_v\alpha_2\delta_1$-dependent processes in mediating modality-specific nociception.

Interestingly, although TSP4-induced dorsal horn neuron sensitization and behavioral hypersensitivity is a slow process that requires 4 days to reach the peak effects, gabapentin at a clinically relevant concentration can block these effects within 1 h. Even through we cannot rule out the possibility that a mechanism independent of its binging to $Ca_v\alpha_2\delta_1$ mediates the actions of gabapentin in reversing TSP4-induced dorsal spinal cord neuron sensitization and behavioral hyperalgesia, our data support that keeping the TSP4/$Ca_v\alpha_2\delta_1$-dependent processes in an active state is probably critical for the maintenance of TSP4-induced central sensitization and behavioral hypersensitivity. The fast anti-hyperalgesia actions of gabapentin may derive from interfering with the TSP4/$Ca_v\alpha_2\delta_1$-dependent processes that are likely key elements of pain genesis even after long term pathological changes, such as aberrant excitatory presynaptic input and synaptogenesis, are established post-TSP4 injection or peripheral nerve injury. This may explain why gabapentinoids exhibit inhibitory effects on sensitized spinal neurons (33, 70, 71) and neuropathic pain states in animal models (24, 25, 72–74) and patients (19–21, 75–82) but do not affect baseline sensory neuron excitability and sensory thresholds in control animals (33, 70, 71, 73, 83) and healthy volunteers (84, 85), who should not have increased expression of $Ca_v\alpha_2\delta_1$ and/or TSP4 in the sensory pathway. This may also explain why gabapentin is only effective in some, but not all, neuropathic pain patients with various etiologies (32) as it is less likely that all pain-inducing conditions are associated with increased expression of $Ca_v\alpha_2\delta_1$ and/or TSP4.

In summary, even though some details remained elusive, our findings provide a large body of multidimensional evidence to support that activation of the TSP4/$Ca_v\alpha_2\delta_1$-dependent processes is required for TSP4-induced central sensitization that leads to pain state development. Blocking this pathway may be a novel strategy for development of target-specific analgesics for chronic pain management.

*Author Contributions*—J. P. designed, performed, and analyzed experiments of *in vitro* binding, immunoprecipitation, protein expression, and purification. Y. P. Y. designed, performed, and analyzed experiments of confocal imaging and synaptogenesis. C.-Y. Z. designed, performed, and analyzed experiments of electrophysiology. K.-W. L., E. C., D.-S. K., B. V., X. Z., and N. G. designed, performed, and analyzed experiments of transgenic animal models and behavioral pharmacology. I. V. and E. P.-R. designed and constructed the shRNA-AAV vectors for the behavioral pharmacology experiments. K. S. and O. S. designed, performed, and analyzed experiments of motor functions. D. W. and G. F. designed, generated, and analyzed the conditional knockout mice. C. E. and B. B. provided the TSP4 KO mice and contributed to conception of the study. F. Z. designed and constructed the TSP4 expression vectors, assisted in protein purification, and contributed to conception of the study. Z. D. L. conceived and coordinated the study. Z. D. L., J. P., Y. P. Y., C.-Y. Z., and E. P.-R. contributed to preparation of the figures and writing the paper. Z. D. L., J. P., Y. P. Y., C.-Y. Z., O. S., C. E., and B. B. contributed to editing of the paper. All authors reviewed the results and approved the final version of the manuscript.

*Acknowledgments—We thank Dr. Diane Lipscombe for the tsA-201 cell lines, Dr. Fan Wang for the Advillin-Cre mice, and Drs. Anatoly Kiyatkin, Ping Deng, Zao Xu, and Joshua Lee for assistance in some initial experiments.*

**References**

1. Pan, B., Yu, H., Park, J., Yu, Y. P., Luo, Z. D., and Hogan, Q. H. (2015) Painful nerve injury up-regulates thrombospondin-4 expression in dorsal root ganglia. *J. Neurosci. Res.* **93,** 443–453
2. Kim, D. S., Li, K. W., Boroujerdi, A., Peter Yu, Y., Zhou, C. Y., Deng, P., Park, J., Zhang, X., Lee, J., Corpe, M., Sharp, K., Steward, O., Eroglu, C., Barres, B., Zaucke, F., Xu, Z. C., and Luo, Z. D. (2012) Thrombospondin-4 contributes to spinal sensitization and neuropathic pain states. *J. Neurosci.* **32,** 8977–8987
3. Adams, J. C. (2001) Thrombospondins: multifunctional regulators of cell interactions. *Annu. Rev. Cell Dev. Biol.* **17,** 25–51
4. Bornstein, P. (2001) Thrombospondins as matricellular modulators of cell function. *J. Clin. Invest.* **107,** 929–934
5. Adams, J. C., and Lawler, J. (2004) The thrombospondins. *Int. J. Biochem. Cell Biol.* **36,** 961–968
6. Arber, S., and Caroni, P. (1995) Thrombospondin-4, an extracellular matrix protein expressed in the developing and adult nervous system promotes neurite outgrowth. *J. Cell Biol.* **131,** 1083–1094
7. Xu, J., Xiao, N., and Xia, J. (2010) Thrombospondin 1 accelerates synap-

togenesis in hippocampal neurons through neuroligin 1. *Nat. Neurosci.* **13,** 22–24
8. Eroglu, C., Allen, N. J., Susman, M. W., O'Rourke, N. A., Park, C. Y., Ozkan, E., Chakraborty, C., Mulinyawe, S. B., Annis, D. S., Huberman, A. D., Green, E. M., Lawler, J., Dolmetsch, R., Garcia, K. C., Smith, S. J., Luo, Z. D., Rosenthal, A., Mosher, D. F., and Barres, B. A. (2009) Gabapentin receptor $\alpha_2\delta_1$ is a neuronal thrombospondin receptor responsible for excitatory CNS synaptogenesis. *Cell* **139,** 380–392
9. Qin, N., Yagel, S., Momplaisir, M. L., Codd, E. E., and D'Andrea, M. R. (2002) Molecular cloning and characterization of the human voltage-gated calcium channel $\alpha_2\delta$-4 subunit. *Mol. Pharmacol.* **62,** 485–496
10. Klugbauer, N., Lacinová, L., Marais, E., Hobom, M., and Hofmann, F. (1999) Molecular diversity of the calcium channel $\alpha2\delta$ subunit. *J. Neurosci.* **19,** 684–691
11. Ellis, S. B., Williams, M. E., Ways, N. R., Brenner, R., Sharp, A. H., Leung, A. T., Campbell, K. P., McKenna, E., Koch, W. J., and Hui, A. (1988) Sequence and expression of mRNAs encoding the $\alpha1$ and $\alpha2$ subunits of a DHP-sensitive calcium channel. *Science* **241,** 1661–1664
12. Bernstein, G. M., and Jones, O. T. (2007) Kinetics of internalization and degradation of N-type voltage-gated calcium channels: role of the $\alpha_2/\delta$ subunit. *Cell Calcium* **41,** 27–40
13. Davies, A., Hendrich, J., Van Minh, A. T., Wratten, J., Douglas, L., and Dolphin, A. C. (2007) Functional biology of the $\alpha_2\delta$ subunits of voltage-gated calcium channels. *Trends Pharmacol. Sci.* **28,** 220–228
14. Hoppa, M. B., Lana, B., Margas, W., Dolphin, A. C., and Ryan, T. A. (2012) $\alpha2\delta$ expression sets presynaptic calcium channel abundance and release probability. *Nature* **486,** 122–125
15. Davies, A., Kadurin, I., Alvarez-Laviada, A., Douglas, L., Nieto-Rostro, M., Bauer, C. S., Pratt, W. S., and Dolphin, A. C. (2010) The $\alpha2\delta$ subunits of voltage-gated calcium channels form GPI-anchored proteins, a posttranslational modification essential for function. *Proc. Natl. Acad. Sci. U.S.A.* **107,** 1654–1659
16. Klugbauer, N., Marais, E., and Hofmann, F. (2003) Calcium channel $\alpha2\delta$ subunits: differential expression, function, and drug binding. *J. Bioenerg. Biomembr.* **35,** 639–647
17. Gee, N. S., Brown, J. P., Dissanayake, V. U., Offord, J., Thurlow, R., and Woodruff, G. N. (1996) The novel anticonvulsant drug, gabapentin (Neurontin), binds to the $\alpha2\delta$ subunit of a calcium channel. *J. Biol. Chem.* **271,** 5768–5776
18. Marais, E., Klugbauer, N., and Hofmann, F. (2001) Calcium channel $\alpha2\delta$ subunits-structure and gabapentin binding. *Mol. Pharmacol.* **59,** 1243–1248
19. Backonja, M., and Glanzman, R. L. (2003) Gabapentin dosing for neuropathic pain: evidence from randomized, placebo-controlled clinical trials. *Clin. Ther.* **25,** 81–104
20. Dworkin, R. H., and Kirkpatrick, P. (2005) Pregabalin. *Pregabalin. Nat. Rev. Drug Discov.* **4,** 455–456
21. Guay, D. R. (2005) Pregabalin in neuropathic pain: a more "pharmaceutically elegant" gabapentin? *Am. J. Geriatr. Pharmacother.* **3,** 274–287
22. Zareba, G. (2005) Pregabalin: a new agent for the treatment of neuropathic pain. *Drugs Today* **41,** 509–516
23. Hwang, J. H., and Yaksh, T. L. (1997) Effect of subarachnoid gabapentin on tactile-evoked allodynia in a surgically induced neuropathic pain model in the rat. *Reg. Anesth.* **22,** 249–256
24. Luo, Z. D., Calcutt, N. A., Higuera, E. S., Valder, C. R., Song, Y. H., Svensson, C. I., and Myers, R. R. (2002) Injury type-specific calcium channel $\alpha_2\delta_1$ subunit up-regulation in rat neuropathic pain models correlates with antiallodynic effects of gabapentin. *J. Pharmacol. Exp. Ther.* **303,** 1199–1205
25. Luo, Z. D., Chaplan, S. R., Higuera, E. S., Sorkin, L. S., Stauderman, K. A., Williams, M. E., and Yaksh, T. L. (2001) Up-regulation of dorsal root ganglion $\alpha_2\delta$ calcium channel subunit and its correlation with allodynia in spinal nerve-injured rats. *J. Neurosci.* **21,** 1868–1875
26. Field, M. J., Cox, P. J., Stott, E., Melrose, H., Offord, J., Su, T. Z., Bramwell, S., Corradini, L., England, S., Winks, J., Kinloch, R. A., Hendrich, J., Dolphin, A. C., Webb, T., and Williams, D. (2006) Identification of the $\alpha_2\delta_1$ subunit of voltage-dependent calcium channels as a molecular target for pain mediating the analgesic actions of pregabalin. *Proc. Natl. Acad. Sci. U.S.A.* **103,** 17537–17542
27. Bauer, C. S., Nieto-Rostro, M., Rahman, W., Tran-Van-Minh, A., Ferron, L., Douglas, L., Kadurin, I., Sri Ranjan, Y., Fernandez-Alacid, L., Millar, N. S., Dickenson, A. H., Lujan, R., and Dolphin, A. C. (2009) The increased trafficking of the calcium channel subunit $\alpha_2\delta_1$ to presynaptic terminals in neuropathic pain is inhibited by the $\alpha_2\delta$ ligand pregabalin. *J. Neurosci.* **29,** 4076–4088
28. Li, K. W., Yu, Y. P., Zhou, C., Kim, D. S., Lin, B., Sharp, K., Steward, O., and Luo, Z. D. (2014) Calcium channel $\alpha_2\delta_1$ proteins mediate trigeminal neuropathic pain states associated with aberrant excitatory synaptogenesis. *J. Biol. Chem.* **289,** 7025–7037
29. Li, C. Y., Song, Y. H., Higuera, E. S., and Luo, Z. D. (2004) Spinal dorsal horn calcium channel $\alpha_2\delta_1$ subunit up-regulation contributes to peripheral nerve injury-induced tactile allodynia. *J. Neurosci.* **24,** 8494–8499
30. Zhou, C., and Luo, Z. D. (2015) Nerve injury-induced calcium channel $\alpha_2\delta_1$ protein dysregulation leads to increased pre-synaptic excitatory input into deep dorsal horn neurons and neuropathic allodynia. *Eur. J. Pain* **19,** 1267–1276
31. Newton, R. A., Bingham, S., Case, P. C., Sanger, G. J., and Lawson, S. N. (2001) Dorsal root ganglion neurons show increased expression of the calcium channel $\alpha_2\delta_1$ subunit following partial sciatic nerve injury. *Brain Res. Mol. Brain Res.* **95,** 1–8
32. Gordh, T. E., Stubhaug, A., Jensen, T. S., Arnèr, S., Biber, B., Boivie, J., Mannheimer, C., Kalliomäki, J., and Kalso, E. (2008) Gabapentin in traumatic nerve injury pain: a randomized, double-blind, placebo-controlled, cross-over, multi-center study. *Pain* **138,** 255–266
33. Zhou, C., and Luo, Z. D. (2014) Electrophysiological characterization of spinal neuron sensitization by elevated calcium channel $\alpha_2\delta_1$ subunit protein. *Eur. J. Pain* **18,** 649–658
34. Li, C. Y., Zhang, X. L., Matthews, E. A., Li, K. W., Kurwa, A., Boroujerdi, A., Gross, J., Gold, M. S., Dickenson, A. H., Feng, G., and Luo, Z. D. (2006) Calcium channel $\alpha_2\delta_1$ subunit mediates spinal hyperexcitability in pain modulation. *Pain* **125,** 20–34
35. Hasegawa, H., Abbott, S., Han, B. X., Qi, Y., and Wang, F. (2007) Analyzing somatosensory axon projections with the sensory neuron-specific Advillin gene. *J. Neurosci.* **27,** 14404–14414
36. Södersten, F., Ekman, S., Schmitz, M., Paulsson, M., and Zaucke, F. (2006) Thrombospondin-4 and cartilage oligomeric matrix protein form heterooligomers in equine tendon. *Connect Tissue Res* **47,** 85–91
37. Pan, J. Q., and Lipscombe, D. (2000) Alternative splicing in the cytoplasmic II-III loop of the N-type Ca channel $\alpha$ 1B subunit: functional differences are $\beta$ subunit-specific. *J. Neurosci.* **20,** 4769–4775
38. Jönsson, U., Fägerstam, L., Ivarsson, B., Johnsson, B., Karlsson, R., Lundh, K., Löfås, S., Persson, B., Roos, H., and Rönnberg, I. (1991) Real-time biospecific interaction analysis using surface plasmon resonance and a sensor chip technology. *BioTechniques* **11,** 620–627
39. Johnsson, B., Löfås, S., and Lindquist, G. (1991) Immobilization of proteins to a carboxymethyldextran-modified gold surface for biospecific interaction analysis in surface plasmon resonance sensors. *Anal. Biochem.* **198,** 268–277
40. Lin, Y., McDonough, S. I., and Lipscombe, D. (2004) Alternative splicing in the voltage-sensing region of N-type CaV2.2 channels modulates channel kinetics. *J. Neurophysiol.* **92,** 2820–2830
41. Kim, S. H., and Chung, J. M. (1992) An experimental model for peripheral neuropathy produced by segmental spinal nerve ligation in the rat. *Pain* **50,** 355–363
42. Rigaud, M., Gemes, G., Barabas, M. E., Chernoff, D. I., Abram, S. E., Stucky, C. L., and Hogan, Q. H. (2008) Species and strain differences in rodent sciatic nerve anatomy: implications for studies of neuropathic pain. *Pain* **136,** 188–201
43. Chang, K., Elledge, S. J., and Hannon, G. J. (2006) Lessons from nature: microRNA-based shRNA libraries. *Nat. Methods* **3,** 707–714
44. Chung, K. H., Hart, C. C., Al-Bassam, S., Avery, A., Taylor, J., Patel, P. D., Vojtek, A. B., and Turner, D. L. (2006) Polycistronic RNA polymerase II expression vectors for RNA interference based on BIC/miR-155. *Nucleic Acids Res.* **34,** e53
45. McCarty, D. M., Monahan, P. E., and Samulski, R. J. (2001) Self-complementary recombinant adeno-associated virus (scAAV) vectors promote

efficient transduction independently of DNA synthesis. *Gene Ther.* **8,** 1248–1254
46. Hioki, H., Kameda, H., Nakamura, H., Okunomiya, T., Ohira, K., Nakamura, K., Kuroda, M., Furuta, T., and Kaneko, T. (2007) Efficient gene transduction of neurons by lentivirus with enhanced neuron-specific promoters. *Gene Ther.* **14,** 872–882
47. Ma, D., Zerangue, N., Lin, Y. F., Collins, A., Yu, M., Jan, Y. N., and Jan, L. Y. (2001) Role of ER export signals in controlling surface potassium channel numbers. *Science* **291,** 316–319
48. Shepard, A. R., Jacobson, N., and Clark, A. F. (2005) Importance of quantitative PCR primer location for short interfering RNA efficacy determination. *Anal. Biochem.* **344,** 287–288
49. Boroujerdi, A., Zeng, J., Sharp, K., Kim, D., Steward, O., and Luo, Z. D. (2011) Calcium channel $\alpha_2\delta_1$ protein up-regulation in dorsal spinal cord mediates spinal cord injury-induced neuropathic pain states. *Pain* **152,** 649–655
50. Kim, D. S., Figueroa, K. W., Li, K. W., Boroujerdi, A., Yolo, T., and Luo, Z. D. (2009) Profiling of dynamically changed gene expression in dorsal root ganglia post peripheral nerve injury and a critical role of injury-induced glial fibrillary acidic protein in maintenance of pain behaviors [corrected]. *Pain* **143,** 114–122
51. Dixon, W. J. (1980) Efficient analysis of experimental observations. *Annu. Rev. Pharmacol. Toxicol.* **20,** 441–462
52. Hargreaves, K., Dubner, R., Brown, F., Flores, C., and Joris, J. (1988) A new and sensitive method for measuring thermal nociception in cutaneous hyperalgesia. *Pain* **32,** 77–88
53. Randall, L. O., and Selitto, J. J. (1957) A method for measurement of analgesic activity on inflamed tissue. *Arch. Int. Pharmacodyn. Ther.* **111,** 409–419
54. Basso, D. M., Fisher, L. C., Anderson, A. J., Jakeman, L. B., McTigue, D. M., and Popovich, P. G. (2006) Basso mouse scale for locomotion detects differences in recovery after spinal cord injury in five common mouse strains. *J. Neurotrauma* **23,** 635–659
55. Jay, S. D., Sharp, A. H., Kahl, S. D., Vedvick, T. S., Harpold, M. M., and Campbell, K. P. (1991) Structural characterization of the dihydropyridine-sensitive calcium channel α2-subunit and the associated delta peptides. *J. Biol. Chem.* **266,** 3287–3293
56. Graham, B. A., Brichta, A. M., and Callister, R. J. (2007) Moving from an averaged to specific view of spinal cord pain processing circuits. *J. Neurophysiol.* **98,** 1057–1063
57. Braz, J., Solorzano, C., Wang, X., and Basbaum, A. I. (2014) Transmitting pain and itch messages: a contemporary view of the spinal cord circuits that generate gate control. *Neuron* **82,** 522–536
58. Shimoyama, M., Shimoyama, N., and Hori, Y. (2000) Gabapentin affects glutamatergic excitatory neurotransmission in the rat dorsal horn. *Pain* **85,** 405–414
59. Nguyen, D., Deng, P., Matthews, E. A., Kim, D. S., Feng, G., Dickenson, A. H., Xu, Z. C., and Luo, Z. D. (2009) Enhanced pre-synaptic glutamate release in deep-dorsal horn contributes to calcium channel $\alpha_2\delta_1$ protein-mediated spinal sensitization and behavioral hypersensitivity. *Mol. Pain* **5,** 6
60. Michalski, D., Härtig, W., Krügel, K., Edwards, R. H., Böddener, M., Böhme, L., Pannicke, T., Reichenbach, A., and Grosche, A. (2013) Region-specific expression of vesicular glutamate and GABA transporters under various ischaemic conditions in mouse forebrain and retina. *Neuroscience* **231,** 328–344
61. Perederiy, J. V., Luikart, B. W., Washburn, E. K., Schnell, E., and Westbrook, G. L. (2013) Neural injury alters proliferation and integration of adult-generated neurons in the dentate gyrus. *J. Neurosci.* **33,** 4754–4767
62. Faralli, A., Dagna, F., Albera, A., Bekku, Y., Oohashi, T., Albera, R., Rossi, F., and Carulli, D. (2015) Modifications of perineuronal nets and remodelling of excitatory and inhibitory afferents during vestibular compensation in the adult mouse. *Brain Struct Funct.* 10.1007/s00429-015-1095-7
63. Underhill, S. M., Wheeler, D. S., and Amara, S. G. (2015) Differential regulation of two isoforms of the glial glutamate transporter EAAT2 by DLG1 and CaMKII. *J. Neurosci.* **35,** 5260–5270
64. Nikitczuk, J. S., Patil, S. B., Matikainen-Ankney, B. A., Scarpa, J., Shapiro, M. L., Benson, D. L., and Huntley, G. W. (2014) N-cadherin regulates molecular organization of excitatory and inhibitory synaptic circuits in adult hippocampus *in vivo*. *Hippocampus* **24,** 943–962
65. Ben-Menachem, E., Söderfelt, B., Hamberger, A., Hedner, T., and Persson, L. I. (1995) Seizure frequency and CSF parameters in a double-blind placebo controlled trial of gabapentin in patients with intractable complex partial seizures. *Epilepsy Res.* **21,** 231–236
66. Rose, M. A., and Kam, P. C. A. (2002) Gabapentin: pharmacology and its use in pain management. *Anaesthesia* **57,** 451–462
67. Chang, E. Y., Chen, X., Sandhu, A., Li, C. Y., and Luo, Z. D. (2013) Spinal 5-HT3 receptors facilitate behavioural hypersensitivity induced by elevated calcium channel $\alpha_2\delta_1$ protein. *Eur. J. Pain* **17,** 505–513
68. Dunkle, E. T., Zaucke, F., and Clegg, D. O. (2007) Thrombospondin-4 and matrix three-dimensionality in axon outgrowth and adhesion in the developing retina. *Exp. Eye Res.* **84,** 707–717
69. Park, J., Trinh, V. N., Sears-Kraxberger, I., Li, K. W., Steward, O., and Luo, Z. D. (2016) Synaptic ultrastructure changes in trigeminocervical complex posttrigeminal nerve injury. *J. Comp. Neurol.* **524,** 309–322
70. Stanfa, L. C., Singh, L., Williams, R. G., and Dickenson, A. H. (1997) Gabapentin, ineffective in normal rats, markedly reduces C-fibre evoked responses after inflammation. *Neuroreport* **8,** 587–590
71. Patel, M. K., Gonzalez, M. I., Bramwell, S., Pinnock, R. D., and Lee, K. (2000) Gabapentin inhibits excitatory synaptic transmission in the hyperalgesic spinal cord. *Br. J. Pharmacol.* **130,** 1731–1734
72. Xiao, W., Boroujerdi, A., Bennett, G. J., and Luo, Z. D. (2007) Chemotherapy-evoked painful peripheral neuropathy: Analgesic effects of gabapentin and effects on expression of the $\alpha_2\delta$ type-1 calcium channel subunit. *Neuroscience* **144,** 714–720
73. Hunter, J. C., Gogas, K. R., Hedley, L. R., Jacobson, L. O., Kassotakis, L., Thompson, J., and Fontana, D. J. (1997) The effect of novel anti-epileptic drugs in rat experimental models of acute and chronic pain. *Eur. J. Pharmacol.* **324,** 153–160
74. Abdi, S., Lee, D. H., and Chung, J. M. (1998) The anti-allodynic effects of amitriptyline, gabapentin, and lidocaine in a rat model of neuropathic pain. *Anesth. Analg.* **87,** 1360–1366
75. To, T. P., Lim, T. C., Hill, S. T., Frauman, A. G., Cooper, N., Kirsa, S. W., and Brown, D. J. (2002) Gabapentin for neuropathic pain following spinal cord injury. *Spinal Cord* **40,** 282–285
76. Stacey, B. R., Dworkin, R. H., Murphy, K., Sharma, U., Emir, B., and Griesing, T. (2008) Pregabalin in the treatment of refractory neuropathic pain: results of a 15-month open-label trial. *Pain Med.* **9,** 1202–1208
77. Levendoglu F., Ogün, C. O., Ozerbil O, Ogün, T. C., Ugurlu, H. (2004) Gabapentin is a first line drug for the treatment of neuropathic pain in spinal cord injury. *Spine* **29,** 743–751
78. Backonja, M., Beydoun, A., Edwards, K. R., Schwartz, S. L., Fonseca, V., Hes, M., LaMoreaux, L., and Garofalo, E. (1998) Gabapentin for the symptomatic treatment of painful neuropathy in patients with diabetes mellitus: a randomized controlled trial (see comments). *JAMA* **280,** 1831–1836
79. Ahn, S. H., Park, H. W., Lee, B. S., Moon, H. W., Jang, S. H., Sakong, J., and Bae, J. H. (2003) Gabapentin effect on neuropathic pain compared among patients with spinal cord injury and different durations of symptoms. *Spine* **28,** 341–346
80. Dworkin, R. H., O'Connor, A. B., Backonja, M., Farrar, J. T., Finnerup, N. B., Jensen, T. S., Kalso, E. A., Loeser, J. D., Miaskowski, C., Nurmikko, T. J., Portenoy, R. K., Rice, A. S., Stacey, B. R., Treede, R. D., Turk, D. C., and Wallace, M. S. (2007) Pharmacologic management of neuropathic pain: evidence-based recommendations. *Pain* **132,** 237–251
81. Rosenberg, J. M., Harrell, C., Ristic, H., Werner, R. A., and de Rosayro, A. M. (1997) The effect of gabapentin on neuropathic pain. *Clin. J. Pain* **13,** 251–255
82. Rosner, H., Rubin, L., and Kestenbaum, A. (1996) Gabapentin adjunctive therapy in neuropathic pain states. *Clin. J. Pain* **12,** 56–58
83. Field, M. J., Oles, R. J., Lewis, A. S., McCleary, S., Hughes, J., and Singh, L. (1997) Gabapentin (neurontin) and *S*-(+)-3-isobutylgaba represent a novel class of selective antihyperalgesic agents. *Brit. J. Pharmacol.* **121,** 1513–1522
84. Werner, M. U., Perkins, F. M., Holte, K., Pedersen, J. L., and Kehlet, H. (2001) Effects of gabapentin in acute inflammatory pain in humans. *Reg. Anesth. Pain Med.* **26,** 322–328
85. Gustorff, B., Hoechtl, K., Sycha, T., Felouzis, E., Lehr, S., and Kress, H. G. (2004) The effects of remifentanil and gabapentin on hyperalgesia in a new extended inflammatory skin pain model in healthy volunteers. *Anesth. Analg.* **98,** 401–407